

Original Article

Difference in oral microbiota composition between patients with stage 5 chronic kidney disease on hemodialysis and healthy controls

Yumian Gan^{1,2*}, Dandan Ruan^{1,2*}, Quanzuan Zeng^{1*}, Yaobin Zhu⁴, Yanan Hu¹, Rong Wu¹, Xinfu Lin¹, Jiabin Wu¹, Xiaorong Meng¹, Jiewei Luo¹, Meizhu Gao^{1,2}, Xin Chen^{1,3}

¹Fujian Provincial Hospital, Shengli Clinical Medical College of Fujian Medical University, Fuzhou 350001, Fujian, China; ²Nephrology Department, Fujian Provincial Hospital, Fuzhou 350001, Fujian, China; ³Pathology Department, Fujian Provincial Hospital, Fuzhou 350001, Fujian, China; ⁴Department of Traditional Chinese Medicine, The First Affiliated Hospital, Fujian Medical University, Fuzhou 350003, Fujian, China. *Equal contributors.

Received October 20, 2022; Accepted February 17, 2023; Epub May 15, 2023; Published May 30, 2023

Abstract: Owing to the symbiotic relationship between the microbiota and the human body, the microbiome is considered a “second human genome”. Microorganisms are inextricably associated with human diseases and can affect the host phenotype. In the present study, 25 female patients with stage 5 chronic kidney disease (CKD5) undergoing hemodialysis in our hospital and 25 healthy subjects were recruited. The structure of the oral microbiota of the study participants was analyzed using the MiSeq PE300 sequencing platform and high-throughput 16S rDNA sequencing. The microbiota was compared between the groups using QIIME and the stats package in R. In total, 1,336 operational taxonomic units (OTUs) were obtained, and the relative frequencies of 450 OTUs differed significantly between the two groups ($P < 0.05$), indicating that the samples were rich in OTUs. A comparison of β -diversity indicated a significant difference in the microbial community structure between the two groups ($P < 0.05$). These results indicated that the biological diversity of the oral microbiota was highly correlated with CKD5. In this experiment, 189 genera, with significant differences in abundance between the groups ($P < 0.05$), were found. Furthermore, differences in the structure of the oral microbiota were observed between the groups at the phylum, class, order, family, and genus levels. Collectively, an imbalance in the oral microbiota may accelerate the progression of CKD and cause additional complications.

Keywords: Stage 5 chronic kidney disease, hemodialysis, oral microbiota, 16S rDNA sequencing, immune imbalance

Introduction

Lederberg et al. [1] proposed the concept of the human microbiome, which is the general term for the symbiotic and pathogenic microorganisms in the ecological community found in or on the human body. Owing to the symbiotic relationship, the microbiome is considered a “second human genome” and has been studied extensively. Generally, human genes include genes in both the human genome and the microbiome; thus, the metabolic functions of humans have characteristics of both humans and microorganisms. Microorganisms are inextricably linked to human diseases and phenotypic variation. Many microorganisms can be

found in the oral cavity, and the oral mucosa consistently interacts with several microorganisms. The oral cavity contains the most microorganisms in the human body after the intestine. Interactions among oral microbes contribute to the response to adverse external stimuli. Imbalances in the microbiota can lead to oral diseases, such as dental caries and periodontitis [2], mucosal diseases, and other systemic diseases [3], such as those of the gastrointestinal and nervous systems [4]. Thus, the oral microbiota plays an important role in human microbial communities and human health [5].

An imbalance in the intestinal microbiota in patients with stage 5 chronic kidney disease

(CKD5) receiving hemodialysis (HD) has been clearly demonstrated [6]. Additionally, the oral cavity is the main entry site of the gastrointestinal tract, and oral pathogenic microorganisms induce disruptions in the intestinal microflora in animal models [7]. A previous study has shown that the content of periodontal pathogens in patients with end-stage renal disease is higher than that in non-CKD controls [8, 9]. The periodontal tissue of adolescent patients with CKD not receiving dialysis is destroyed, resulting in a change in the oral microbiota [10]; however, the degree of periodontal lesions increases in patients undergoing dialysis, resulting in a step-by-step change in the oral microbiota. When categorizing patients with CKD into hemodialysis, continuous peritoneal dialysis, and non-dialysis treatment groups [11], the severity of periodontal disease was the greatest in the CKD group, with substantial changes in the degree of periodontal disease and the oral microbiota in the hemodialysis group [11]. In the first study on the relation of serum antibodies with oral pathogenic microorganisms and renal function, Kshirsagar et al. found that the serum IgG levels against various pathogens, including *Porphyromonas gingivalis*, *Treponema denticola*, *Haemophilus*, and *Actinomyces*, in the abnormal oral microbiota were negatively correlated with the glomerular filtration rate, a measure of renal damage [12].

In this study, we analyzed the composition of the oral salivary flora and metabolic profiles in patients with CKD and healthy controls. We determined the main microbial taxa in the oral cavity of patients with CKD and the effect of hemodialysis on the microbiota. These results provide a theoretical basis for the regulation of the oral microbiota during adjuvant treatment for CKD.

Materials and methods

Diagnostic, inclusion, and exclusion criteria

CKD was diagnosed if one of the diagnostic criteria was met [33]. The inclusion criteria of CKD5 hemodialysis were: 1) patients (aged > 20 years) were diagnosed with CKD5 and received regular dialysis therapy for more than 3 years (three times per week). 2) patients received regular phosphorus binder treatment, and all individuals resided in local areas and had similar eating habits. The exclusion criteria

were as follows: 1) oral infections, inflammation, pustules, ulcers, benign or malignant masses, and other oral diseases; 2) the use of antibiotics, Niaoduqing, or other preparations containing catharsis ingredients within 4 weeks before sampling; 3) a family history of genetic kidney diseases; 4) smoking and drinking habits; 5) inability to communicate and cooperate normally; 6) history of autoimmune diseases with tumors, acute and chronic infections, and active diseases; 7) blood transfusion in the past 3 months and the use of adrenal cortex hormones and immunosuppressive agents within the past 2 weeks; and 8) lack of complete soft tissues (including the gums, oral mucosa, tongue, pharynx, and tonsils) or missing more than eight teeth for any reason. The inclusion criteria of controls were as follows: 1) eGFR > 90 mL/(min·1.73 m²); 2) there was no abnormality in routine urine and renal imaging; 3) no history of chronic diseases (hypertension, diabetes, hyperuricemia and rheumatic immune diseases) that cause damage to the kidney; 4) no history of kidney transplantation; 5) no active inflammation; 6) no antibacterial drugs and immunosuppressants have been used within 3 months, and there was no obvious infection of viruses, bacteria or fungi and other pathogens.

Saliva sample collection and DNA extraction

Pre-dialysis patients were not allowed to eat, drink, smoke, or chew gum 30 min before sampling. The mouth was rinsed with drinking water. The saliva was retained in the mouth for at least 1 min and repeatedly collected in a sterilized centrifuge tube. Once a sufficient volume of saliva (2-5 mL) was obtained, the sample was centrifuged at 3000 rpm for 15 min. The supernatant was then discarded and the remaining sample was quickly frozen in liquid nitrogen and stored at -80°C. For salivary microbial genome extraction, the 16S rRNA universal primer-341F/806R-was used for PCR amplification of the extracted DNA. The 341F/806R primers were synthesized by Lifetech/Thermo.

Sequencing of the V3-V4 region of the 16S rRNA gene

After PCR amplification, product purification, and inspect of the library quality, Qubit was used for library quantification. Mixing and

homogenization were carried out according to the data volume requirements for each sample. 16S-specific primers were used to amplify the V3-V4 region, and an amplified fragment of approximately 425 bp was obtained. After the adapter was added, Illumina MiSeq was used for sequencing. PANDAseq (V2.9) was used to assemble paired-end reads [34]. After splicing, a long base sequence (clean read) was obtained for the 16S rRNA analysis. The sequencing primers for bacterial 16S rDNA were U341 (CCTACGGGRSGCAGCAG) and U806 (GGACTA-CVGGGTATCTAATC) [35, 36]. Sequencing was performed by Shanghai Applied Protein Technology Co., Ltd. (Shanghai, China).

Operational taxonomic unit clustering

To facilitate the analysis of species diversity, long reads were clustered into OTUs. Clean reads were classified based on unique sequence tags. The abundance of each tag was determined (i.e., read counts were obtained), and then tags were sorted according to their abundance. Clustering was performed with a similarity threshold of 0.97. After chimera filtering of the clustered sequences, the OTUs were obtained, and all clean reads were aligned to the OTU sequence [37]. Using the Greengenes database, the representative sequence was compared with the 16S DNA of known species. After species classification and annotation of each OTU, the OTU abundance table was obtained [38].

Sample complexity and comparison between groups

QIIME was used to analyze alpha and beta diversity indices [13]. An iterative algorithm was used to calculate the difference between groups based on weighted species classification abundance information and unweighted species classification abundance information and results were visualized using distance-based box plots. The difference between the two groups was analyzed using the Wilcoxon test implemented in the R stats package. The Kruskal test in R was used for comparisons between more than two groups.

Metabolites and correlation analysis

Metabolomics based on UHPLC-Q-TOF MS were used to analyze differences in metabolic profiles between samples. The experimental instruments and reagents used were as fol-

lows: AB Triple TOF 5600/6600 mass spectrometer (AB SCIEX); Agilent 1290 Infinity LC ultra-high pressure liquid chromatograph (Agilent); low-temperature high-speed centrifuge (Eppendorf 5430R); Waters, ACQUITY UPLC BEH Amide 1.7 μm , 2.1 mm \times 100 mm column and Waters, ACQUITY UPLC HSS T3 1.8 μm , 2.1 \times 100 mm column; acetonitrile (Merck, 1499230-935); and ammonium acetate (Sigma, 70221). After data were preprocessed using Pareto-scaling, multi-dimensional statistical analyses were performed, including unsupervised principal component analysis (PCA), supervised partial least-squares discriminant analysis (PLS-DA), and orthogonal partial least-squares discriminant analysis (OPLS-DA). One-dimensional statistical analyses included the Student's *t*-test and multiple analysis of variance. R software was used to construct volcano plots. Spearman correlation coefficients were used to analyze the correlations between microbial taxa with significant differences in abundance and significant differential metabolites. Thereafter, using R and Cytoscape, a matrix heat map was generated and hierarchical clustering, KEGG enrichment analysis, and correlation network analysis were performed. The interactions between microbial taxa and metabolites were explored from multiple perspectives.

Statistical methods

The clinical data of this subject were analyzed using SPSS 20.0 software. The normally distributed measures were expressed as mean \pm standard deviation, and independent samples *t*-test was used for comparison between two groups. The non-normally distributed measures were expressed as median (M) and 25-75% quartiles (Quartiles), and the Two-Sample Kolmogorov-Smirnov test was used for comparison between two groups, while the chi-square test was used for comparison between groups of count data. In addition, flora statistical analysis was performed according to the R language, as described previously. All *P* values were two-tailed, and *P* < 0.05 was considered statistically significant.

Results

General information

A total of 25 patients undergoing hemodialysis with CKD who met the relevant diagnostic and inclusion criteria were enrolled from June 2020

Stage 5 CKD oral microbiota and metabolites

Table 1. Comparison of clinical parameters between the CKD5 hemodialysis group and control group

item	CKD5 hemodialysis group (n=25)	control group (n=25)	F value	P value
Sex (male/female)	13 (52%)/12 (48%)	12 (48.0%)/13 (52.0%)	0.110	0.074
Age (years)	55.56±7.59	54.84±14.223	0.594	0.445
BMI (kg/m ²)	22.21 (17.75-26.33)	23.25 (17.04-28.65)	1.360	0.249
eGFR (mL/(min·1.73m ²))	5.35 (4.37-7.37)	94.10 (80.21-104.40)	4.444	0.000
uric acid (μmol/L)	425.00 (315.00-538.00)	350.50 (292.00-404.50)	1.615	0.011

Note: BMI, Body Mass Index; CKD, Chronic Kidney Disease; eGFR estimate Glomerular Filtration Rate.

to September 2020. A total of 25 healthy controls (12 males and 13 females) were recruited from the physical examination center of our hospital as controls. See **Table 1** for details. This study was approved by the Ethics Committee of Fujian Provincial Hospital in China. The recruited subjects signed the informed consent form.

Operational taxonomic units identification and species abundance analysis

In total, 1,336 operational taxonomic units (OTUs) were obtained from 50 samples ([Supplementary Table 1](#)). Based on species annotation results, histograms for species profiling were generated for each sample at the phylum, class, order, family, and genus levels. A histogram of the relative species abundance can be used to visually evaluate the relative frequencies of taxa in samples at different classification levels (**Figure 1A-E**). According to the species accumulative curve, the sample size was sufficient (**Figure 1F and 1G**).

Alpha diversity analysis

Alpha diversity indices reflect the species diversity of a single sample, including the observed species, Chao1, and phylogene diversity (PD) whole tree indices [13, 14], as well as the Shannon and Simpson indices. A curve that tends to be flat indicates that the amount of sequencing data is sufficient to reflect the microbial information for the sample (**Figure 1F**). The larger the PD whole tree index, the greater the difference in the preservation of the evolutionary history of the species. As determined by rank sum tests (i.e., Kruskal-Wallis tests), the Chao1, PD whole tree, Shannon, Simpson, Goods coverage, and observed species differed significantly between the groups ($P < 0.1$) (**Table 2**).

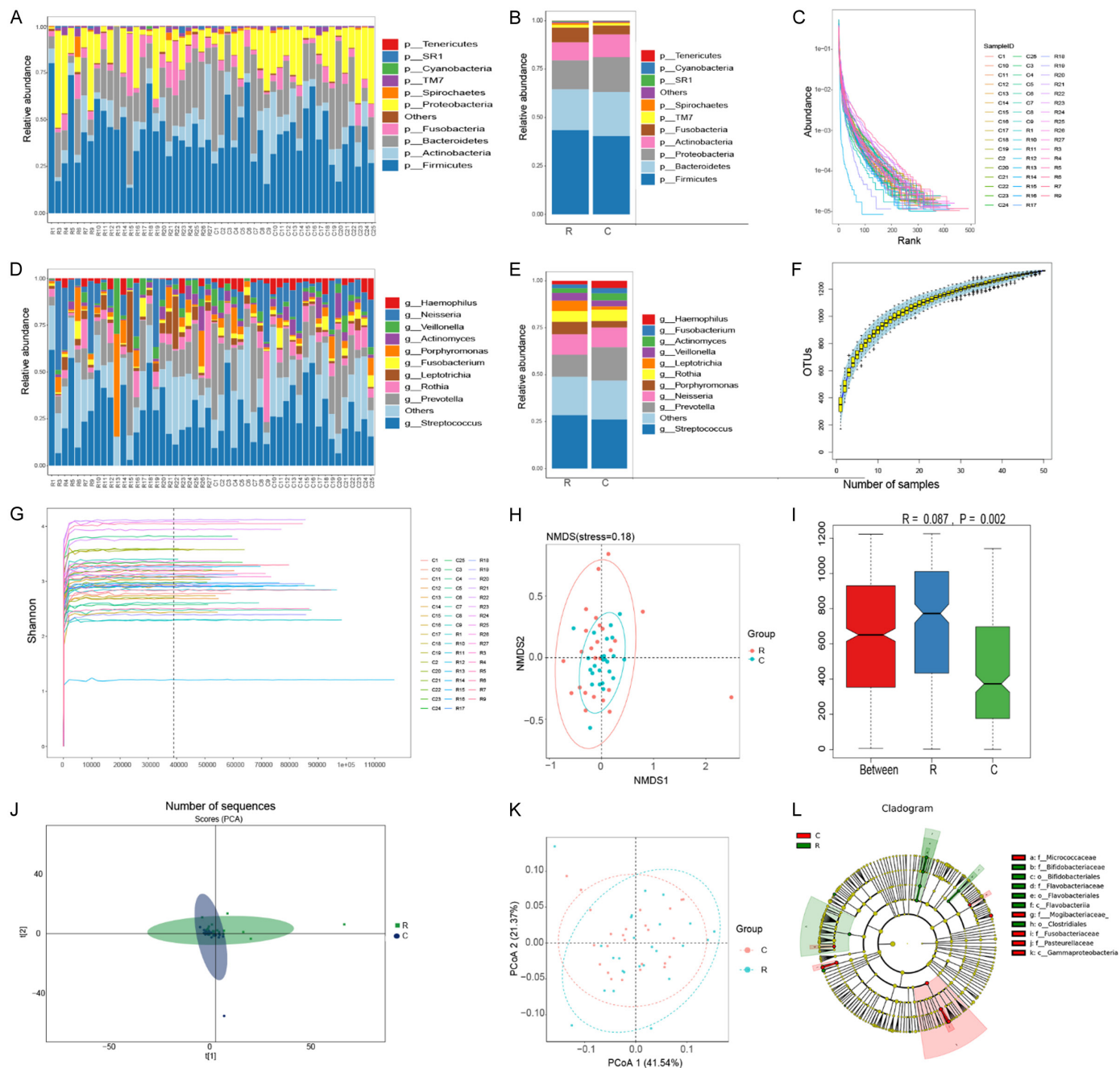
Beta diversity analysis

Beta diversity indicates differences in species diversity between a pair of samples [15]. Beta diversity was compared based on weighted UniFrac distances, indicating a significant difference in the microbial community structure between the two groups ($P < 0.05$) (**Figure 1K**). At the phylum, class, order, family, and genus levels, the differences in species diversity among samples were further evaluated using principal components analysis (PCA), principal coordinates analysis (PCoA), and non-metric multi-dimensional scaling (**Figure 1H, 1J, and 1K**). When two samples are close in these analyses, the species composition of the two samples is similar. ANOSIM also indicated a significant difference between the two groups (**Figure 1I**). The diversity of oral microbes differed substantially between patients with CKD5 undergoing hemodialysis and controls.

Identification of key taxa associated with CKD5

An LDA effect size (LEfSe) analysis was used to estimate the influence of the abundance of each component (species) and determine the communities or species that have a significant effect on sample division. LEfSe analysis emphasizes statistical significance and biological relevance [16]. A phylogeny of species with significant differences is shown in **Figure 1L**. The microbial groups with significant differences in abundance between patients with CKD5 and healthy controls were identified ($P < 0.5$) (**Figure 2A**). The abundance of each biomarker in different groups is shown in [Supplementary Figure 1](#). A STAMP difference analysis, which was used to compare the abundance of species between two sets of samples or multiple sets of samples, indicated a significant difference in oral microbial taxa between the CKD5 group and healthy controls (**Figure 2B-D**).

Stage 5 CKD oral microbiota and metabolites



Stage 5 CKD oral microbiota and metabolites

Figure 1. A. Histogram of the relative abundance of each taxon at the phylum level. B. Relative abundance of species in each group at the phylum level; different colors represent different species. The abscissa represents different samples or groups, the ordinate represents the relative abundance of different species. C. Rank-abundance curve. Abscissa: OTU abundance grade; ordinate: relative frequency of the sequence for the OTU of this grade. The sample ID is displayed on the right. D. Histogram of the relative abundance of each sample at the genus level. E. Histogram of the relative abundance of each group at the phylum level. Different colors represent different species, shown on the right side of the figure. The abscissa represents different samples or groups, and the ordinate represents the relative abundance of different species. F. Species accumulation curves. The abscissa represents the sample size, and the ordinate represents the number of OTUs after sampling. G. Shannon curve. The abscissa represents the number of randomly selected sequence reads, and the ordinate represents the Shannon index. H. Each point represents a sample, and the distance between points represents the degree of difference; samples in the same group are shown in the same color. I. Anosim analysis. Abscissa: Between two groups, and the other two axes showed results within the respective groups. The ordinate represents the rank of the distance between the samples. The *R* value is between (-1, 1); an *R* value greater than 0 indicates a significant difference between groups, whereas an *R* value less than 0 indicates that differences within groups are greater than differences between groups. J. PCA. The abscissa represents the first principal component, the ordinate represents the second principal component, and the percentage represents the contribution to the sample difference. K. PCoA based on weighted UniFrac distances. The abscissa represents the first principal component, and the ordinate represents the second principal component. The percentage represents the contribution to the sample difference. Each point in the figure represents a sample, and different colors represent the group to which the sample belongs. L. Cladogram. The inner-to-outer circles represent the classification from the phylum to genus (or species) level. At different classification levels, each small circle represents a classification at that level, and the diameter is proportional to the relative abundance. Red and green indicate important contributions to different groups; yellow nodes indicate microbial groups that do not play an important role in the two groups. R, patients with stage 5 chronic kidney disease on hemodialysis; C, controls.

Table 2. Comparison of alpha diversity indices between groups (median, M)

Item	CKD 5 hemodialysis group	Control group	Z value	P value
Chao1	451.4819	412.1302	1.414	0.037
Observe	362.0400	336.6400	1.273	0.078
PD whole tree	11.3877	10.6919	0.990	0.012
Shannon	4.4672	4.3440	0.707	0.047
Simpson	0.8784	0.8672	0.849	0.046
Goods coverage	0.9989	0.9986	1.414	0.010

Note: CKD 5, stage 5 Chronic Kidney Disease.

Comparison of metabolites

A typical TIC chromatogram obtained via UHPLC-Q-TOF MS is presented in **Figure 3A-D**. OPLS-DA is a supervised discriminant analysis method. The Q² parameter for our OPLS-DA model was greater than 0.5, and R²Y was close to 1, indicating that the model was stable (**Figure 3E-H**).

The variable importance in projection (VIP) obtained via the OPLS-DA model was used to evaluate the influence of the expression pattern of each metabolite on the classification and determine the differential metabolites with biological significance. The differences between each group were screened with VIP > 1 as the threshold. Univariate statistical analyses were used to verify whether the differences in the metabolites were significant. Metabolites with P < 0.05 were identified as significantly different between the groups and included DL-3-hydroxybutyric acid, trimethylamine N-oxide

(TMAO), and ribitol ([Supplementary Tables 2 and 3](#)). Volcano maps and cluster graph were drawn to visually demonstrate the differences in species at various levels (**Figure 3I and 3J**; [Supplementary Figures 2, 3, 4, 5](#)). A KEGG enrichment analysis revealed that the differential metabolites were related to ABC transporter, central carbon metabolism in cancer, and protein digestion and absorption (**Figure 4A**).

Analysis of correlations between dominant species

A correlation analysis revealed an association between significantly different microbiota and significant metabolites. The groups were clearly distinguished according to metabolomics and microbial diversity. Ten microbial taxa and 172 metabolites with significant differences between the groups were screened ([Supplementary Figure 6](#)). Based on Spearman correlation coefficients, the relationships between taxon abundances and metabolite levels were

Stage 5 CKD oral microbiota and metabolites

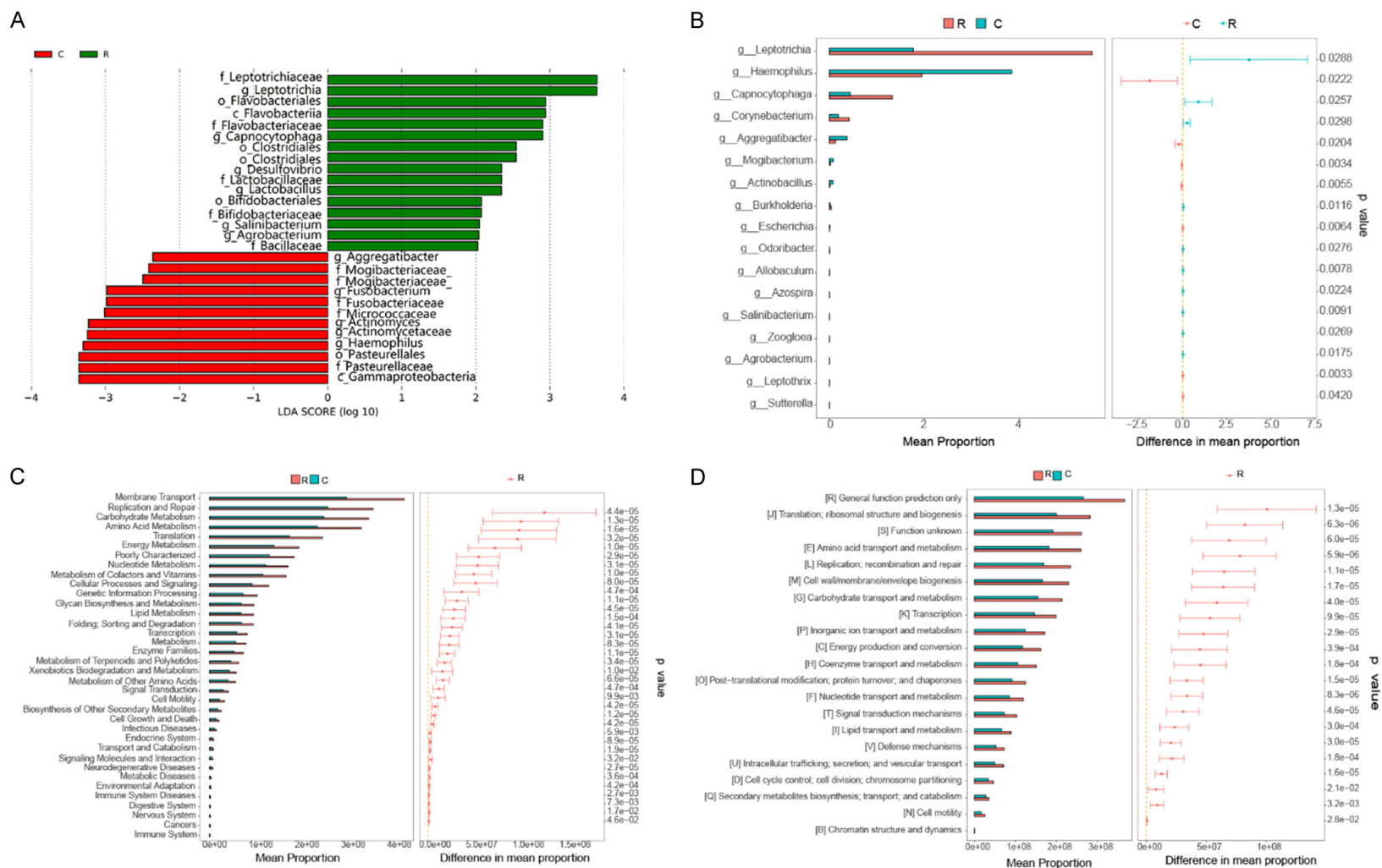


Figure 2. A. LDA score plot. The red and green areas in the LDA score distribution histogram indicate different groups. The figure only shows the species whose LDA score is greater than 2 (the default setting); the length of the bar represents the size of the LDA value. The species names are defined in the legend on the right. B. STAMP difference analysis. Left, abundance ratio of different species in two samples or two groups of samples; middle, proportion of differences within the 95% confidence interval. The value on the right is the *P*-value; *P* < 0.05 indicates a significant difference. C and D. STAMP results using KEGG and COG, respectively. Left, abundance ratio of different functional items in two samples or two groups of samples; middle, difference ratio within the 95% confidence interval; the value on the right is the *P*-value; *P* < 0.05 indicates that the difference is significant. R, patients with stage 5 chronic kidney disease on hemodialysis; C, controls.

Stage 5 CKD oral microbiota and metabolites

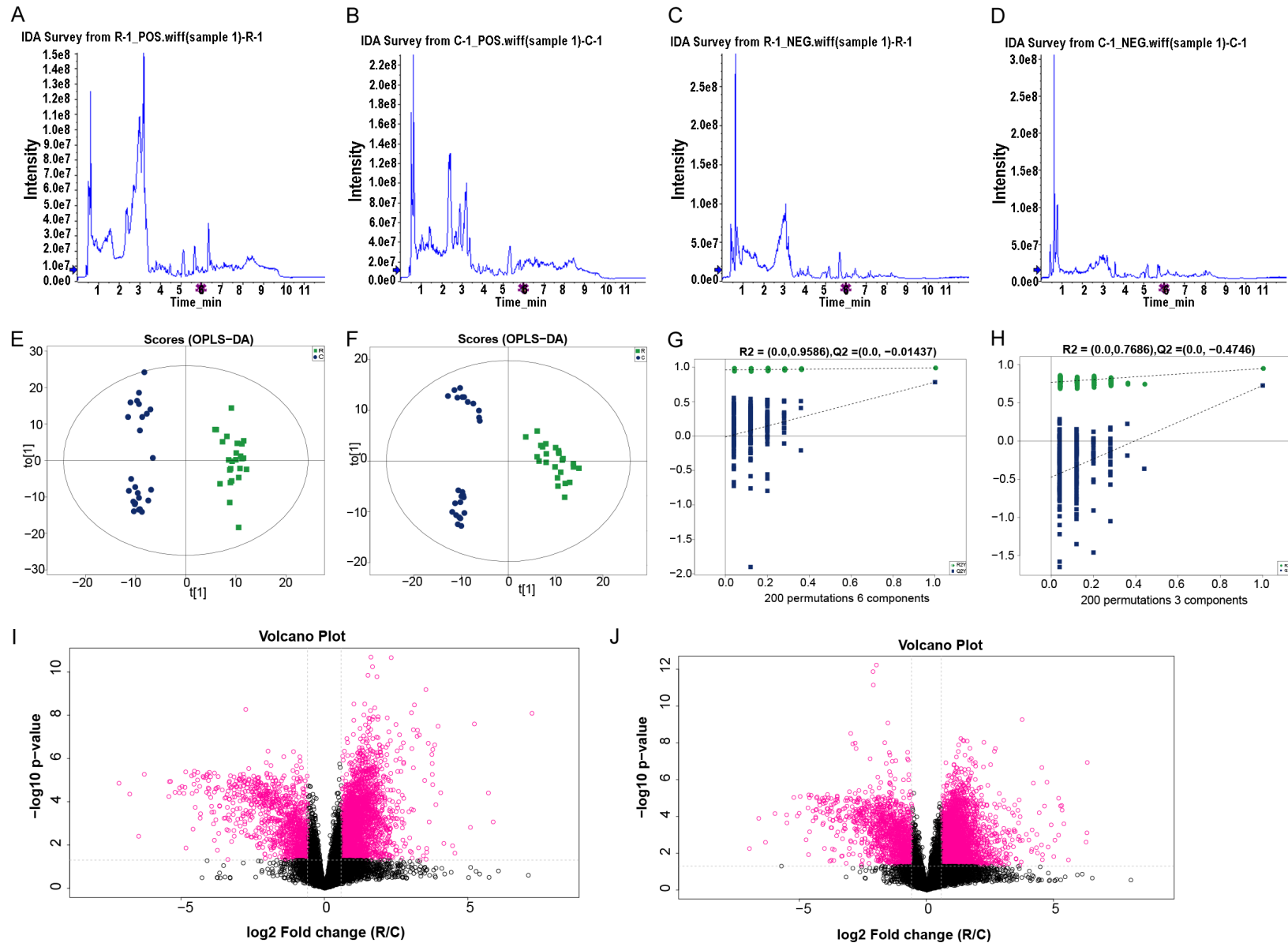


Figure 3. Typical metabolic profiles of samples in each group. A-D. Typical TIC chromatogram obtained by UHPLC-Q-TOF MS. A. Positive ion TIC of samples from the CKD5 group. B. Positive ion TIC of the control sample. C. Negative ion TIC of samples from patients with stage chronic kidney disease. D. Negative ion TIC of the control sample. E and F. OPLS-DA score chart for positive and negative ion mode. G and H. OPLS-DA replacement test for positive and negative ion mode. The abscissa

Stage 5 CKD oral microbiota and metabolites

represents the permutation retention of the permutation test, and the ordinate represents the value of R2 or Q2; all Q2 points from left to right are lower than the original blue Q2 point on the far right, indicating that the model is robust and reliable, without overfitting. I and J. Volcano plot for positive and negative ion modes. The red dots represent metabolites with FC > 1.5 and P < 0.05, which are differential metabolites screened by a univariate statistical analysis. R, patients with stage 5 chronic kidney disease on hemodialysis; C, controls. OPLS-DA, orthogonal partial least-squares discriminant analysis.

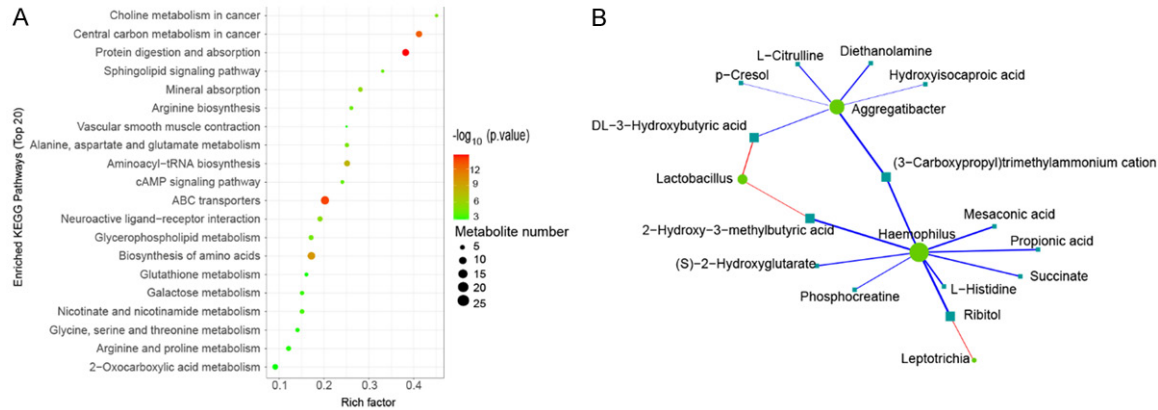


Figure 4. A. KEGG pathway enrichment analysis results. The color of the circle represents the size of the enriched P-value; the size of the dot represents the number of metabolites involved in the corresponding pathway. Ordinate: the metabolic pathway where the target metabolite is enriched; abscissa: enrichment factor. B. Spearman correlation analysis network diagram of significant differential microbiota and metabolites. The circles represent bacterial genera, the rectangles represent significantly differential metabolites. Blue and red represent a positive and negative correlation coefficient; the thickness of the line is proportional to the absolute value of the correlation coefficient. The node size is positively correlated with the degree; the greater the degree, the larger the node size. R, patients with stage 5 chronic kidney disease on hemodialysis; C, controls.

calculated. Three and fifteen pairs of metabolites from the oral microbiota with significant positive and negative correlations, respectively, were found (**Figure 4B**). Using R and Cytoscape, in-depth data mining was performed to evaluate the microbiota and metabolites (**Supplementary Table 4** and **Supplementary Figures 7** and **8**).

Difference in the microbiota between patients with stage 5 chronic kidney disease and healthy controls at the genus level

The relevant bacterial genera (in descending order) with a greater contribution to the CKD5 and hemodialysis group than healthy controls were *Leptotrichia*, *Capnocytophage*, *Corynebacterium*, *Burkholderia*, *Odoribacter*, *Allobaculum*, *Azospira*, *Salinibacterium*, and *Agrobacterium*. The relevant bacteria with a greater contribution to healthy controls (in descending order) than patients were *Haemophilus*, *Aggregatibacter*, *Mogibacterium*, *Actinobacillus*, *Escherichia*, *Leptothrix*, and *Sutterella* (**Figure 2C**).

Discussion

In the present study, 189 bacteria and 172 metabolites with significant differences between groups were identified, providing clear evidence for the imbalance in the oral microbiota in cases of CKD5 and hemodialysis. Notably, in the healthy human oral cavity, *Aggregatibacter* can produce large amounts of lactic acid, which significantly reduces the pH of the oral environment, ultimately inhibiting the growth and reproduction of basophilic pathogens and reducing disease development [17]. *Aggregatibacter* can produce bacteriocins, such as lactosporin and coagulins, key antibacterial substances. The high thermal stability of coagulins contributes to its long-term effects against *Listeria*, *Leuconostoc*, *Pediococcus*, and *Oenococcus*. In addition, coagulins have synergistic beneficial effects with *Lactobacillus* and *Lactococcus*, inhibiting the metabolism of proteins, DNA, and RNA in pathogens [17] and thereby effectively inhibiting the growth and reproduction of pathogenic bacteria. Lactosporin is an anionic antibacterial substance

that can penetrate and destroy the surface of pathogenic bacterial cells. As a result, inorganic salt ions and other substances leak out of the cell, causing the death of pathogenic bacteria. In addition to inhibiting the growth of pathogenic bacteria via bacteriocins, *Bacillus coagulans* can reduce oxidation induced by reactive oxygen species and enhance the macrophage activity of neutrophils [17].

Cell wall components and the fermentation supernatant of *B. coagulans* improve immune and antioxidative activity and promote phagocytosis via the regulation of cytokines [18]. The abundance of *B. coagulans* in patients with CKD5 on hemodialysis was lower than that in healthy controls, suggesting that immunity was weaker in patients than healthy controls. This reduced immune activity makes it easy for various gingival pathogens to enter the blood through the inflamed periodontal tissue, induce systemic inflammation, and accelerate the development of CKD, causing various complications.

Leptotrichia is a genus of non-motile, facultative anaerobic bacterium that mainly exists in the oral cavity but is found in other parts of the human body, including *Lactobacillus labiformis*, *Lactobacillus paleophyllus*, *Lactobacillus hofsiida*, *Lactobacillus hongkongensis*, *Lactobacillus shahai*, *Lactobacillus trevisani*, and *Lactobacillus valedi* [19]. Some species can only grow in the serum or blood. However, all species can ferment carbohydrates and produce lactic acid, which may be related to tooth decay. As opportunistic pathogens, they are involved in various diseases and have been isolated from individuals with immunodeficiency and strong immunity. Mucositis, oral lesions, wounds, and abscesses may easily result in sepsis due to *Trichoderma*. *Capnocytophaga* is a class of microorganisms that can survive under high concentrations of carbon dioxide, parasitize the human oral cavity, and cause oral diseases such as periodontitis [20]. *Corynebacterium* is a gram-positive bacterium that mainly secretes exotoxins. This bacterium usually grows and multiplies on the mucous membrane of the throat and secretes exotoxins, which can cause inflammation and form a gray-white pseudomembrane. After an exotoxin enters the blood, it causes systemic poisoning, often damaging the myocardium and peripheral nerves [20].

According to Kaysen [21], the micro-inflammatory state is a type of immune inflammation not caused by a non-pathogenic microorganism. This state can cause various complications in patients, such as cardiovascular diseases and nutrition-related diseases (e.g., malnutrition and anemia). The mechanism underlying micro-inflammation remains unclear. However, it may be related to dialysis-related factors, abnormal lipid metabolism, bacterial infections (e.g., *Helicobacter pylori*), oxidative stress, kidney factors, immune factors, and various genes.

The micro-inflammatory state can cause changes in certain cytokines, especially inflammatory mediators, such as C-reactive protein (CRP), interleukin (IL), and tumor necrosis factor (TNF). In the state of micro-inflammation, the blood concentration of CRP in the human body increases significantly, consistent with cytokine activation [22]. IL-6 is an autocrine growth factor able to stimulate the proliferation of renal mesangial cells. Studies have shown that an increase in IL-6 levels is positively correlated with the mortality of patients with CKD [23]. Elevated TNF is also an indicator of a micro-inflammatory state [24]. TNF promotes the occurrence and development of inflammation, leading to a cascade of micro-inflammatory reactions in patients with CKD, in turn resulting in various complications. The unique structure of the tooth can promote the deposition of bacterial biofilms, and the excessive accumulation of bacterial biofilms at the gingival margin causes inflammation. The instability of the microbial internal environment promotes the expression of virulence factors, which can lead to local inflammation in periodontal tissues, gingival ulcer formation, and local vascularization. Gingival pathogens can enter the blood through inflamed periodontal tissue and stimulate endothelial cells to express various inflammatory factors. Patients with CKD5 on hemodialysis in this study showed a higher abundance of the genera *Leptotrichia* and *Corynebacterium*, which may result in the development of a micro-inflammatory state, leading to systemic inflammation and various complications.

Interestingly, substantial differential metabolites, e.g., TMAO, were detected in patients with CKD5 on hemodialysis and were produced by differential microbial taxa with differences in abundance between groups, such as *Leptotrichia*, *Capnocytophaga*, and *Salinibacterium*.

Studies have shown [25] that TMAO is a “uremic toxin”. Choline and L-carnitine, which are abundant in red meat and shellfish, are the main raw materials of TMAO. These foods are metabolized to TMA under the action of trimethylamine lyase produced by the intestinal microbiota, and TMAO is generated by the catalysis of flavin-containing monooxygenase 3 (FMO3) in the liver, which is finally eliminated mainly by the kidneys. Studies of a mouse model have revealed that long-term feeding of TMAO or choline can lead to renal fibrosis and increase the levels of renal tubular injury markers [25]. TMAO is a small molecule that can be effectively eliminated by dialysis; however, its harmful effects cannot be ignored. Currently, an increased level of TMAO in the blood of patients with CKD is considered to be related to foam cell formation, atherosclerosis, and cardiovascular events [26] and is an independent predictor of coronary atherosclerosis [27]. Patients of CKD with high blood levels of TMAO have a poor prognosis, a low long-term survival rate, and a high risk of cardiovascular complications [28]. TMAO is also associated with increased insulin resistance [29, 30]. This finding is supported by studies of animal models. Gao et al. [31] revealed that dietary supplementation with TMAO can lead to impaired glucose tolerance in mice and changes in liver insulin signal transduction pathways and promote inflammation in adipose tissue. In addition, insulin inhibits the expression of FMO3 in vitro. In insulin-resistant mice, the knockout of this enzyme inhibited forkhead box O1, a key transcription factor involved in the regulation of insulin signaling [32]. Therefore, high levels of TMAO in patients with CKD5 on hemodialysis may be associated with a high risk of cardiovascular and diabetes-related complications.

Conclusion

CKD5 and hemodialysis were associated with an imbalance in the oral microbiota. This dysregulation of the oral microbiota induced a micro-inflammatory state, causing a systemic inflammatory response and immune disorders. The metabolites of the oral microbiota in patients with CKD5 on hemodialysis were abnormal, including TMAO and N1-MN. These findings were based on sequencing data for clinical samples and bioinformatics analyses, and the results still need to be verified by

functional experiments. The results of this study provide a theoretical basis for the regulation of the oral microbiota during the adjuvant treatment of CKD.

Acknowledgements

This work was supported in part by the Startup Fund for Scientific Research, Fujian Medical University (2019QH1072), Outstanding Youth Project of Fujian Provincial Hospital (2014-YNQN31) and Fujian Province Natural Science Fund Project (2020J011064, 2021J02053). In addition, the clinical studies were supported by national Chinese medicine experts (Zhang Xuemei, Yan Xiaohua) inheritance studio construction project, and the Special Research Foundation of the Fujian Provincial Department of Finance (No. 2020-822, 2021-848, 2021-917), China.

Disclosure of conflict of interest

None.

Abbreviations

BMI, Body Mass Index; CKD, Chronic Kidney Disease; KEGG, Kyoto Encyclopedia of Genes and Genomes; OTU, Operational Taxonomic Unit; PCA, Principal Component Analysis; PCoA, Principal Coordinates Analysis; TMAO, Trimethylamine n-oxide; VIP, Variable Importance in Projection.

Address correspondence to: Jiewei Luo, Meizhu Gao and Xin Chen, Fujian Provincial Hospital, Shengli Clinical Medical College of Fujian Medical University, No. 134 Dongjie, Fuzhou 350001, Fujian, China. E-mail: doclu0421@aliyun.com (JWL); 2505311-94@qq.com (MZG); 729039151@qq.com (XC)

References

- [1] Lederberg J and AT M. ‘Ome sweet’ omics-a genealogical treasury of words genealogical treasury of words. *Scientist* 2001.
- [2] Wasfi R, Abd El-Rahman OA, Zafer MM and Ashour HM. Probiotic lactobacillus sp. inhibit growth, biofilm formation and gene expression of caries-inducing streptococcus mutans. *J Cell Mol Med* 2018; 22: 1972-1983.
- [3] Saikaly SK, Saikaly TS and Saikaly LE. Recurrent aphthous ulceration: a review of potential causes and novel treatments. *J Dermatolog Treat* 2018; 29: 542-552.

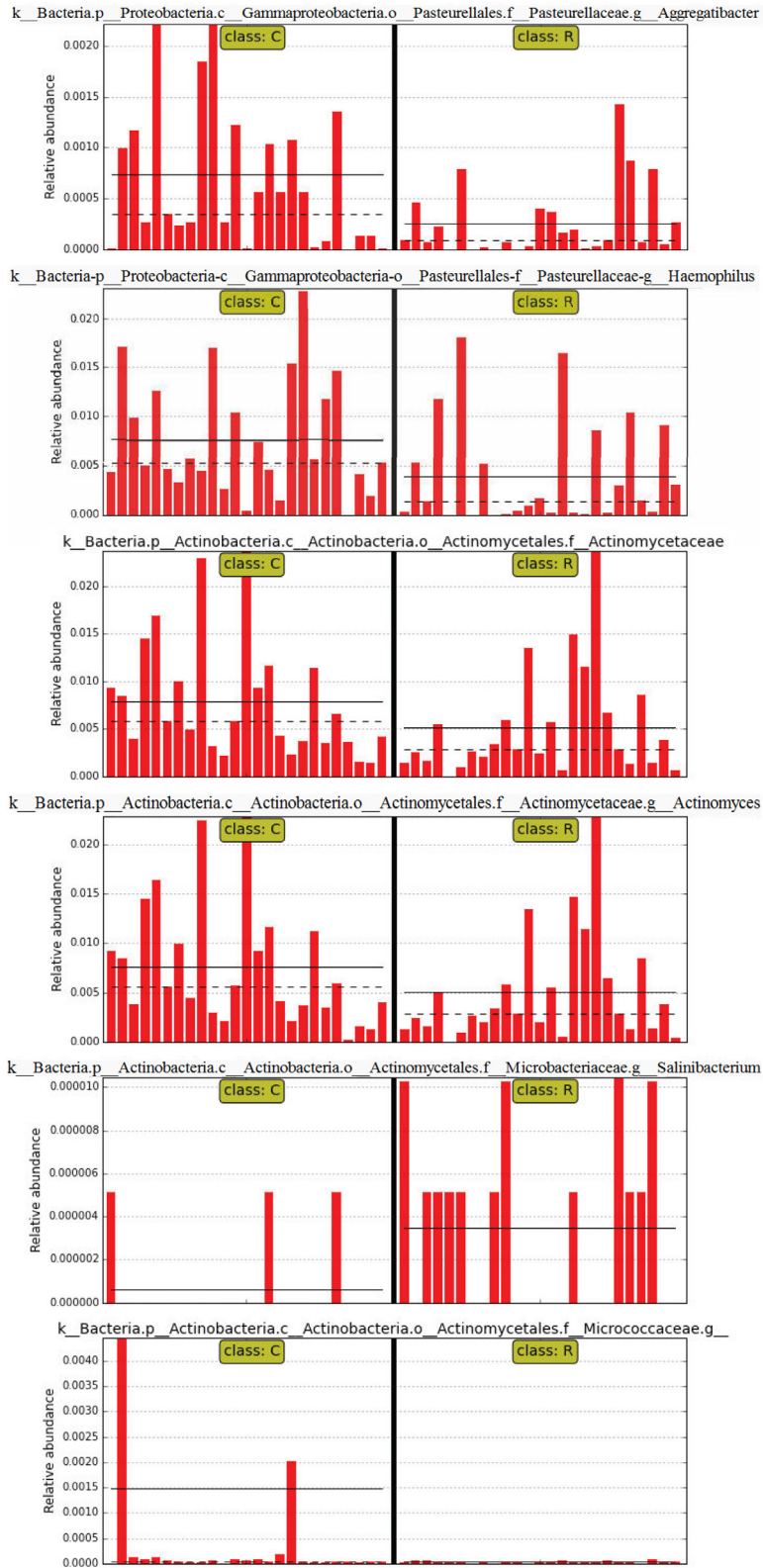
Stage 5 CKD oral microbiota and metabolites

- [4] Lira-Junior R and Boström EA. Oral-gut connection: one step closer to an integrated view of the gastrointestinal tract? *Mucosal Immunol* 2018; 11: 316-318.
- [5] Zarco MF, Vess TJ and Ginsburg GS. The oral microbiome in health and disease and the potential impact on personalized dental medicine. *Oral Dis* 2012; 18: 109-120.
- [6] Vaziri ND, Wong J, Pahl M, Piceno YM, Yuan J, DeSantis TZ, Ni Z, Nguyen TH and Andersen GL. Chronic kidney disease alters intestinal microbial flora. *Kidney Int* 2013; 83: 308-315.
- [7] Araujo MV, Hong BY, Fava PL, Khan S, Burleson JA, Fares G, Samson W, Strausbaugh LD, Diaz PI and Ioannidou E. End stage renal disease as a modifier of the periodontal microbiome. *BMC Nephrol* 2015; 16: 80.
- [8] Nakajima M, Arimatsu K, Kato T, Matsuda Y, Minagawa T, Takahashi N, Ohno H and Yamazaki K. Oral administration of *P. gingivalis* induces dysbiosis of gut microbiota and impaired barrier function leading to dissemination of enterobacteria to the liver. *PLoS One* 2015; 10: e0134234.
- [9] Schmalz G, Kauffels A, Kollmar O, Slotta JE, Vasko R, Muller GA, Haak R and Ziebolz D. Oral behavior, dental, periodontal and microbiological findings in patients undergoing hemodialysis and after kidney transplantation. *BMC Oral Health* 2016; 16: 72.
- [10] Davidovich E, Schwarz Z, Davidovitch M, Eidelman E and Bimstein E. Oral findings and periodontal status in children, adolescents and young adults suffering from renal failure. *J Clin Periodontol* 2005; 32: 1076-1082.
- [11] Borawski J, Wilczyńska-Borawska M, Stokowska W and Myśliwiec M. The periodontal status of pre-dialysis chronic kidney disease and maintenance dialysis patients. *Nephrol Dial Transplant* 2007; 22: 457-464.
- [12] Kshirsagar AV, Offenbacher S, Moss KL, Barros SP and Beck JD. Antibodies to periodontal organisms are associated with decreased kidney function. The dental atherosclerosis risk in communities study. *Blood Purif* 2007; 25: 125-132.
- [13] Kemp PF and Aller JY. Bacterial diversity in aquatic and other environments: what 16S rDNA libraries can tell us. *FEMS Microbiol Ecol* 2004; 47: 161-177.
- [14] Palmer RJ Jr. Composition and development of oral bacterial communities. *Periodontol* 2000 2014; 64: 20-39.
- [15] Yu Z, Yang J, Liu L, Zhang W and Amalfitano S. Bacterioplankton community shifts associated with epipelagic and mesopelagic waters in the Southern Ocean. *Sci Rep* 2015; 5: 12897.
- [16] Segata N, Izard J, Waldron L, Gevers D, Miropolsky L, Garrett WS and Huttenhower C. Metagenomic biomarker discovery and explanation. *Genome Biol* 2011; 12: R60.
- [17] Montville TJ and Bruno ME. Evidence that dissipation of proton motive force is a common mechanism of action for bacteriocins and other antimicrobial proteins. *Int J Food Microbiol* 1994; 24: 53-74.
- [18] Kodali VP and Sen R. Antioxidant and free radical scavenging activities of an exopolysaccharide from a probiotic bacterium. *Biotechnol J* 2008; 3: 245-51.
- [19] Eribe ERK and Olsen I. *Leptotrichia* species in human infections II. *J Oral Microbiol* 2017; 9: 1368848.
- [20] Fernández VA, Juliet LC and Valenzuela MM. *Capnocytophaga*. *Rev Chilena Infectol* 2007; 24: 57-58.
- [21] Kaysen GA. The microinflammatory state in uremia: causes and potential consequences. *J Am Soc Nephrol* 2001; 12: 1549-1557.
- [22] Tspirpanlis G, Chatzipanagiotou S and Nicolaou C. Microinflammation versus inflammation in chronic renal failure patients. *Kidney Int* 2004; 66: 2093-2094.
- [23] Mohangi GU, Singh-Rambirich S and Volchansky A. Periodontal disease: mechanisms of infection and inflammation and possible impact on miscellaneous systemic diseases and conditions. *SADJ* 2013; 68: 462, 464-467.
- [24] Davidovich E, Schwarz Z, Davidovitch M, Eidelman E and Bimstein E. Oral findings and periodontal status in children, adolescents and young adults suffering from renal failure. *J Clin Periodontol* 2005; 32: 1076-1082.
- [25] Wang S, Lv D, Jiang S, Jiang J, Liang M, Hou F and Chen Y. Quantitative reduction in short-chain fatty acids, especially butyrate, contributes to the progression of chronic kidney disease. *Clin Sci (Lond)* 2019; 133: 1857-1870.
- [26] Chen S, Henderson A, Petriello MC, Romano KA, Gearing M, Miao J, Schell M, Sandoval-Espinola WJ, Tao J, Sha B, Graham M, Croke R, Kleinridders A, Balskus EP, Rey FE, Morris AJ and Biddinger SB. Trimethylamine n-oxide binds and activates PERK to promote metabolic dysfunction. *Cell Metab* 2019; 30: 1141-1151, e1145.
- [27] Fu BC, Hullar MAJ, Randolph TW, Franke AA, Monroe KR, Cheng I, Wilkens LR, Shepherd JA, Madeleine MM, Le Marchand L, Lim U and Lampe JW. Associations of plasma trimethylamine N-oxide, choline, carnitine, and betaine with inflammatory and cardiometabolic risk biomarkers and the fecal microbiome in the multiethnic cohort adiposity phenotype study. *Am J Clin Nutr* 2020; 111: 1226-1234.
- [28] Zhang X, Li Y, Yang P, Liu X, Lu L, Chen Y, Zhong X, Li Z, Liu H, Ou C, Yan J and Chen M. Trimethylamine-N-oxide promotes vascular calcifica-

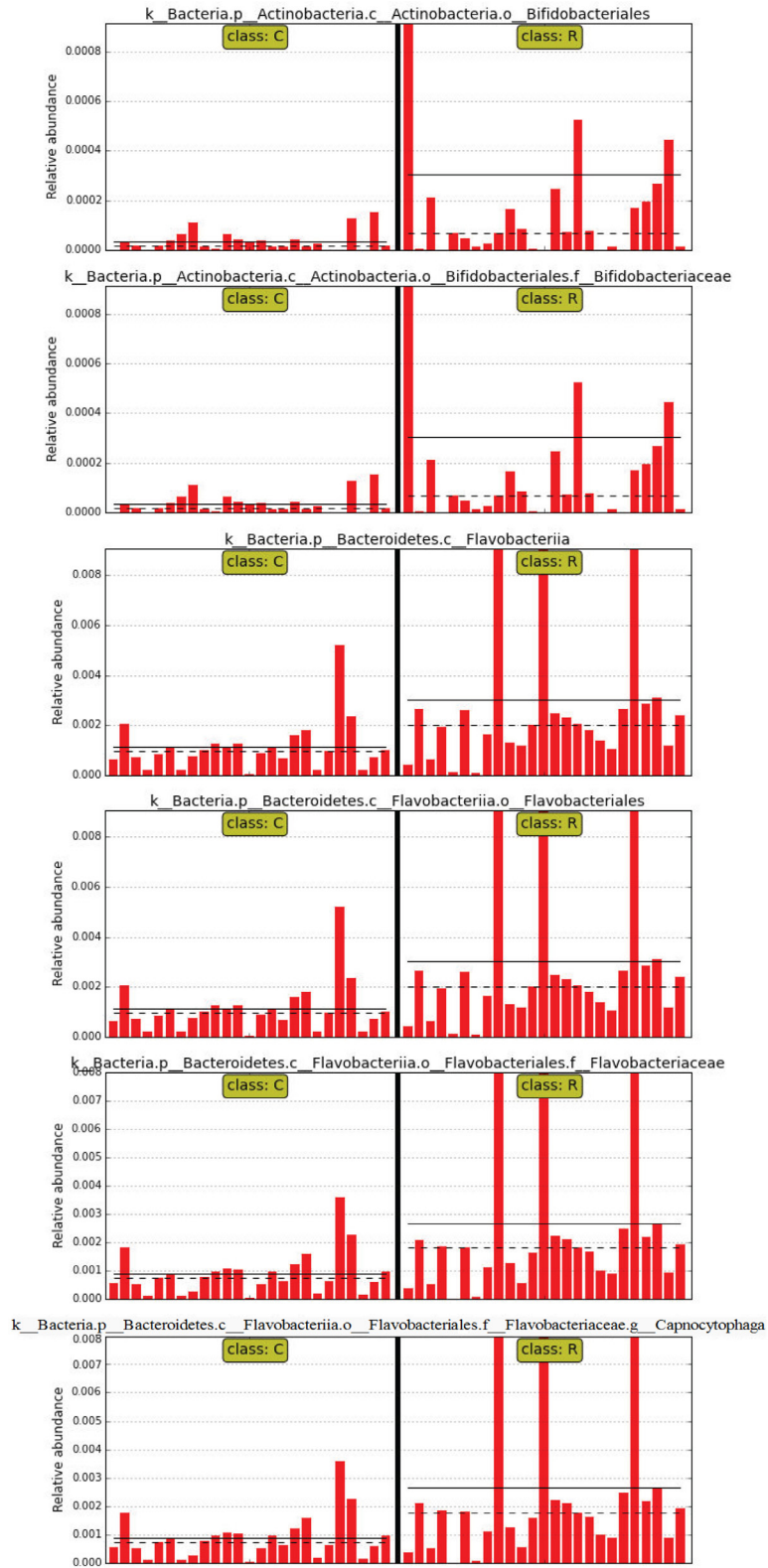
Stage 5 CKD oral microbiota and metabolites

- tion through activation of NLRP3 (nucleotide-binding domain, leucine-rich-containing family, pyrin domain-containing-3) inflammasome and NF- κ B (nuclear factor κ B) signals. *Arterioscler Thromb Vasc Biol* 2020; 40: 751-765.
- [29] Shan Z, Sun T, Huang H, Chen S, Chen L, Luo C, Yang W, Yang X, Yao P, Cheng J, Hu FB and Liu L. Association between microbiota-dependent metabolite trimethylamine-N-oxide and type 2 diabetes. *Am J Clin Nutr* 2017; 106: 888-894.
- [30] Li Y, Wang DD, Chiuve SE, Manson JE, Willett WC, Hu FB and Qi L. Dietary phosphatidylcholine intake and type 2 diabetes in men and women. *Diabetes Care* 2015; 38: e13-14.
- [31] Gao X, Liu X, Xu J, Xue C, Xue Y and Wang Y. Dietary trimethylamine N-oxide exacerbates impaired glucose tolerance in mice fed a high fat diet. *J Biosci Bioeng* 2014; 118: 476-481.
- [32] Miao J, Ling AV, Manthena PV, Gearing ME, Graham MJ, Crooke RM, Croce KJ, Esquejo RM, Clish CB, Morbid Obesity Study G, Vicent D and Biddinger SB. Flavin-containing monooxygenase 3 as a potential player in diabetes-associated atherosclerosis. *Nat Commun* 2015; 6: 6498.
- [33] Levey AS and Coresh J. Chronic kidney disease. *Lancet* 2012; 379: 165-180.
- [34] Masella AP, Bartram AK, Truszkowski JM, Brown DG and Neufeld JD. PANDAseq: paired-end assembler for illumina sequences. *BMC Bioinformatics* 2012; 13: 31.
- [35] Wang Y and Qian PY. Conservative fragments in bacterial 16S rRNA genes and primer design for 16S ribosomal DNA amplicons in metagenomic studies. *PLoS One* 2009; 4: e7401.
- [36] Zakrzewski M, Goesmann A, Jaenicke S, Junemann S, Eikmeyer F, Szczepanowski R, Al-Soud WA, Sorensen S, Puhler A and Schluter A. Profiling of the metabolically active community from a production-scale biogas plant by means of high-throughput metatranscriptome sequencing. *J Biotechnol* 2012; 158: 248-258.
- [37] Edgar RC. UPARSE: highly accurate OTU sequences from microbial amplicon reads. *Nat Methods* 2013; 10: 996-998.
- [38] Cole JR, Wang Q, Fish JA, Chai B, McGarrell DM, Sun Y, Brown CT, Porras-Alfaro A, Kuske CR and Tiedje JM. Ribosomal database project: data and tools for high throughput rRNA analysis. *Nucleic Acids Res* 2014; 42: D633-642.

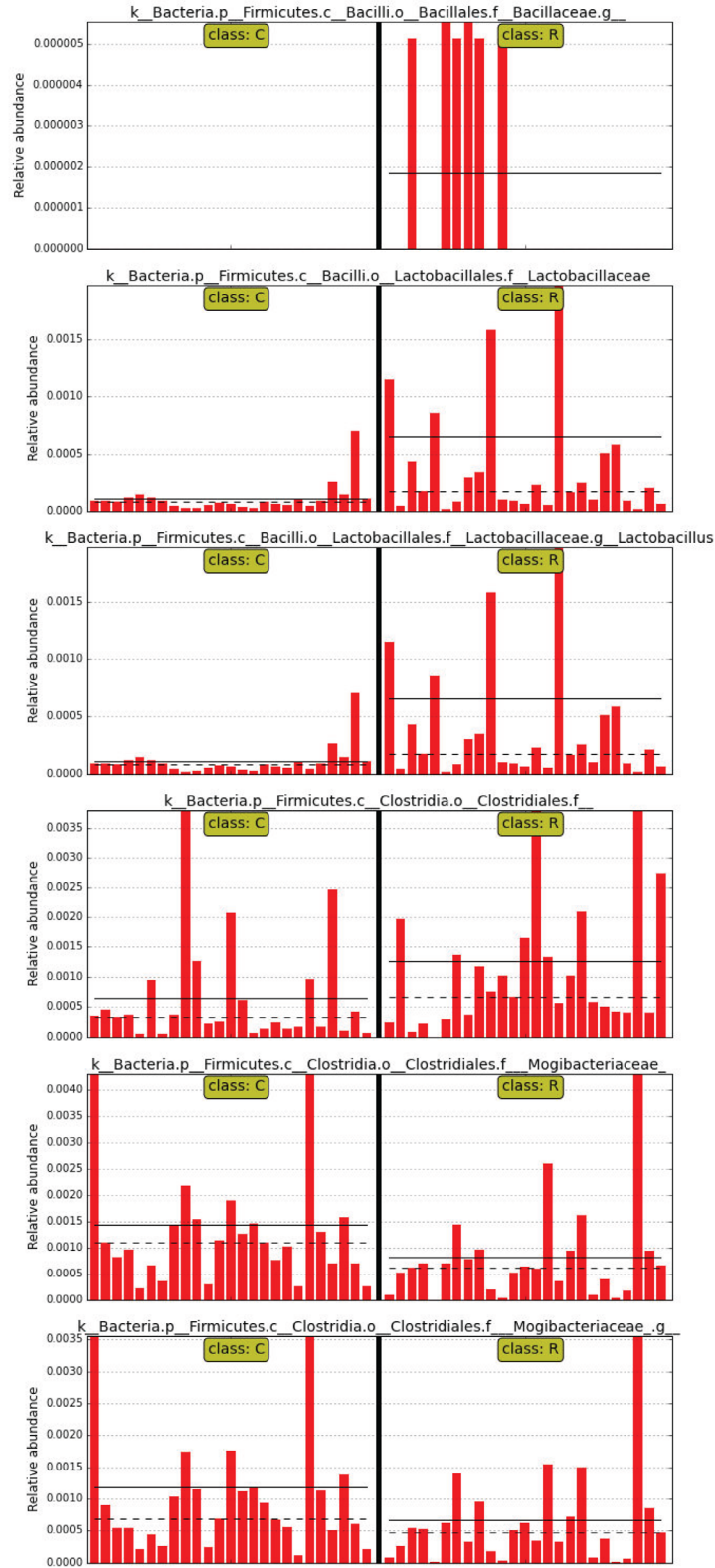
Stage 5 CKD oral microbiota and metabolites



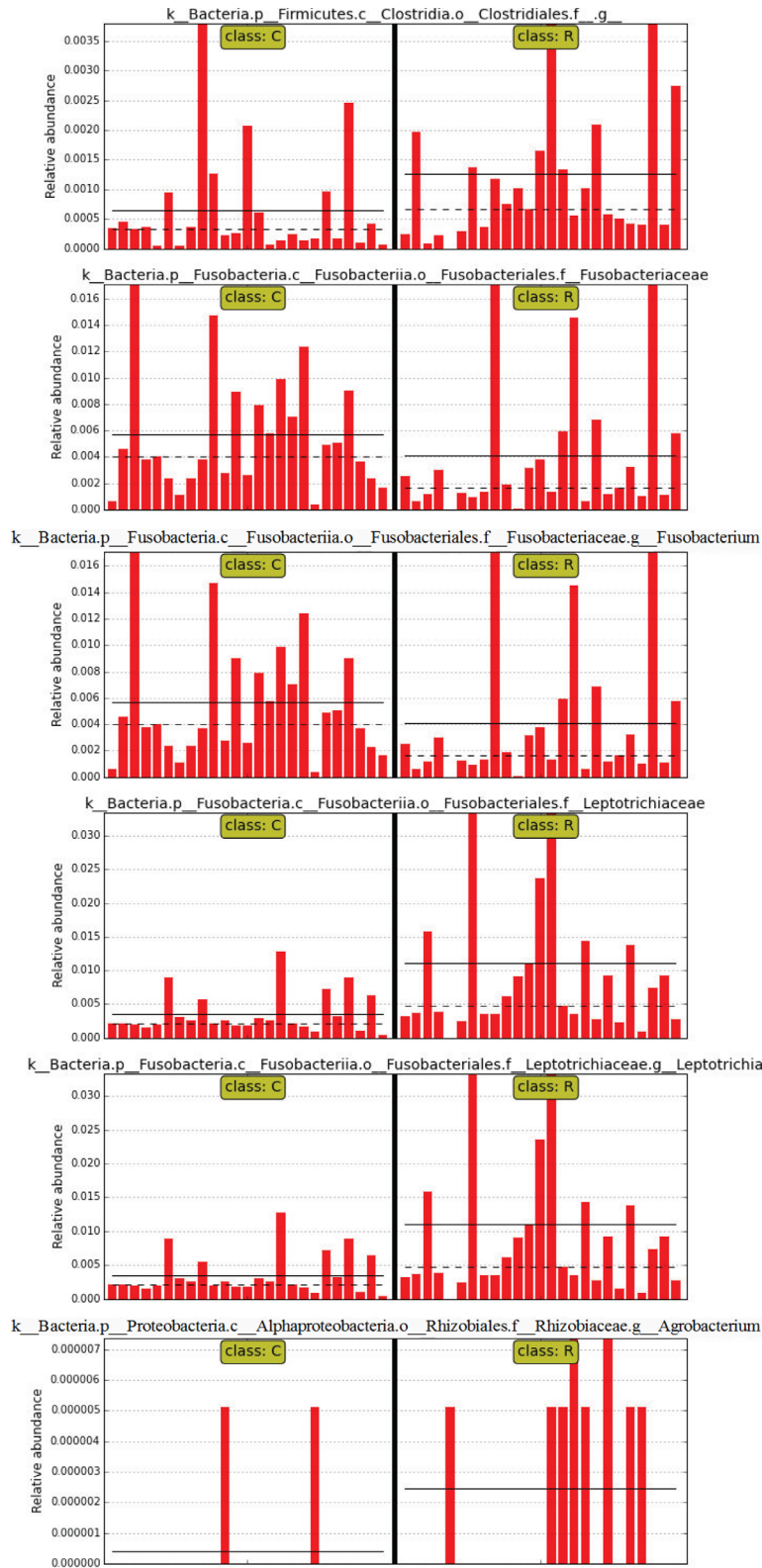
Stage 5 CKD oral microbiota and metabolites



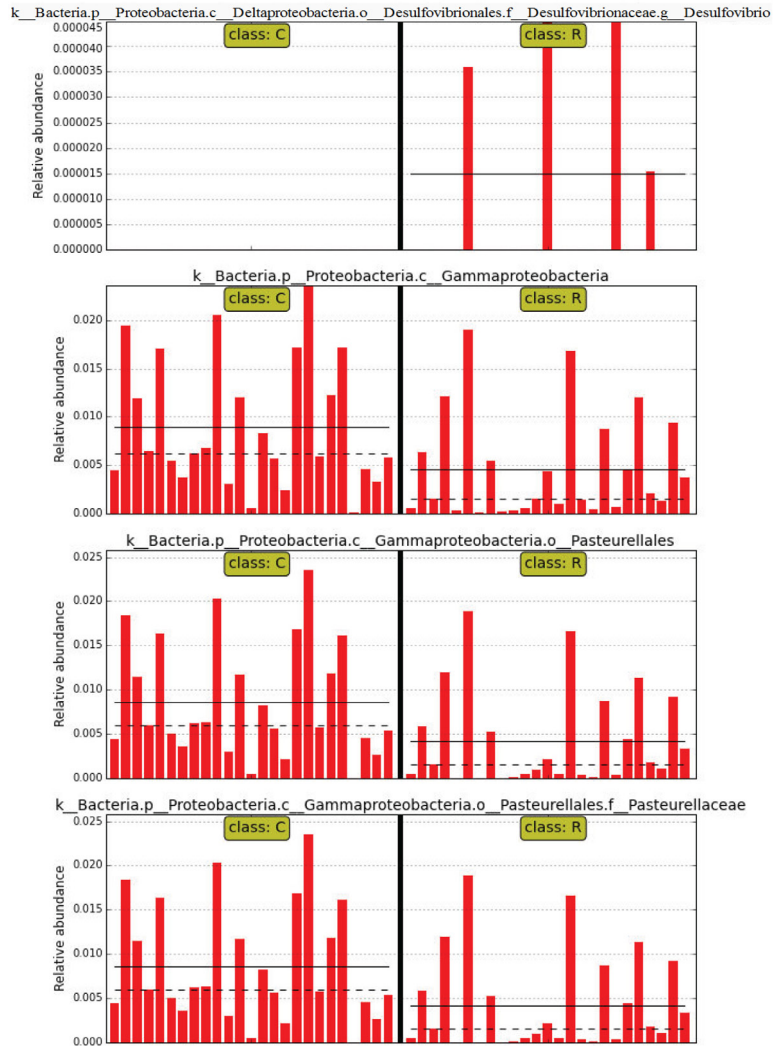
Stage 5 CKD oral microbiota and metabolites



Stage 5 CKD oral microbiota and metabolites



Stage 5 CKD oral microbiota and metabolites



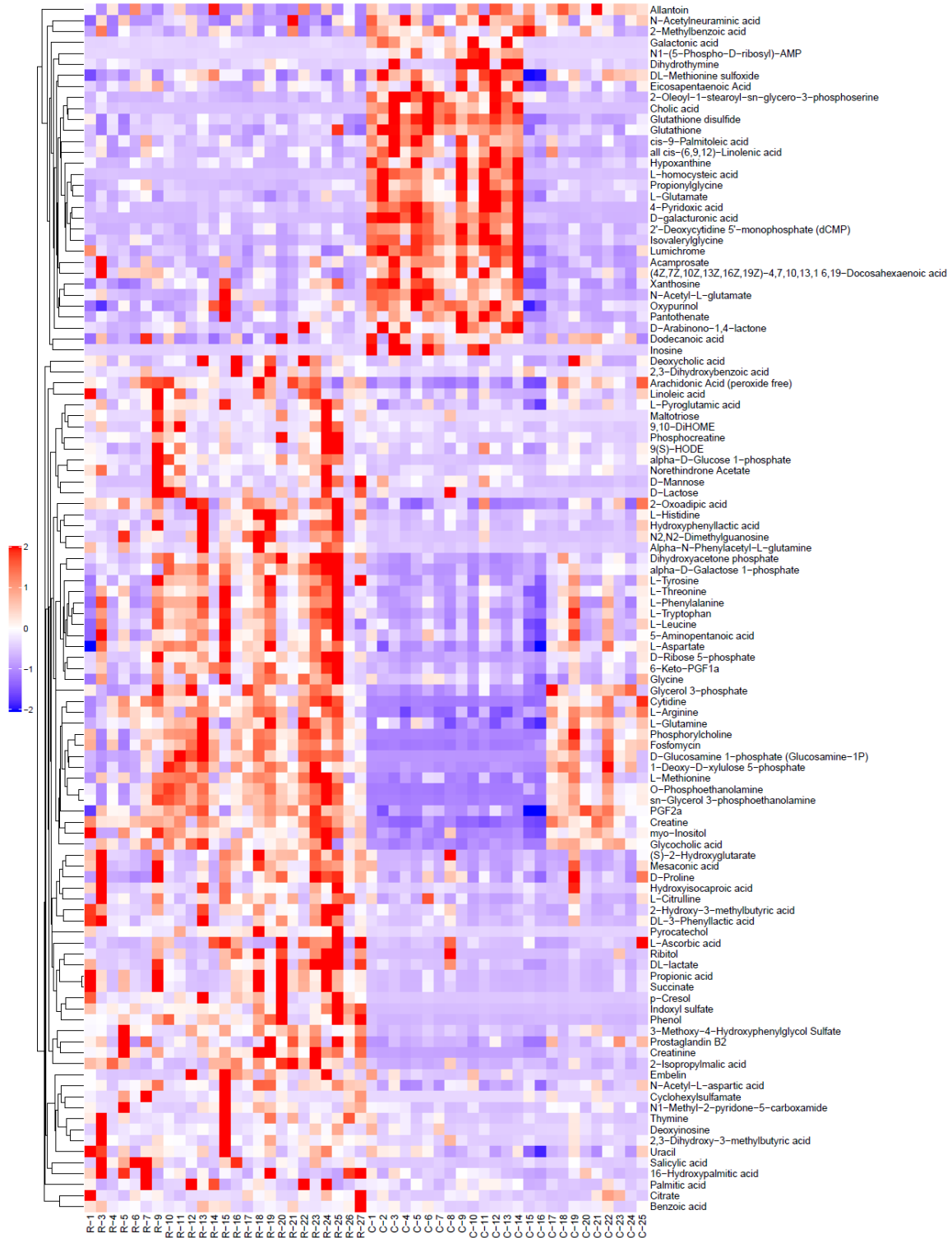
Supplementary Figure 1. The abundance comparison chart of each biomarker in different groups. Species with a default LDA value greater than two are biomarkers with statistical differences between groups. The left and right sides of the figure indicate different groups. The abscissa represents the sample; the ordinate represents the relative abundance of bacteria. R, stage 5 chronic kidney disease patients on hemodialysis; C, controls.

Stage 5 CKD oral microbiota and metabolites



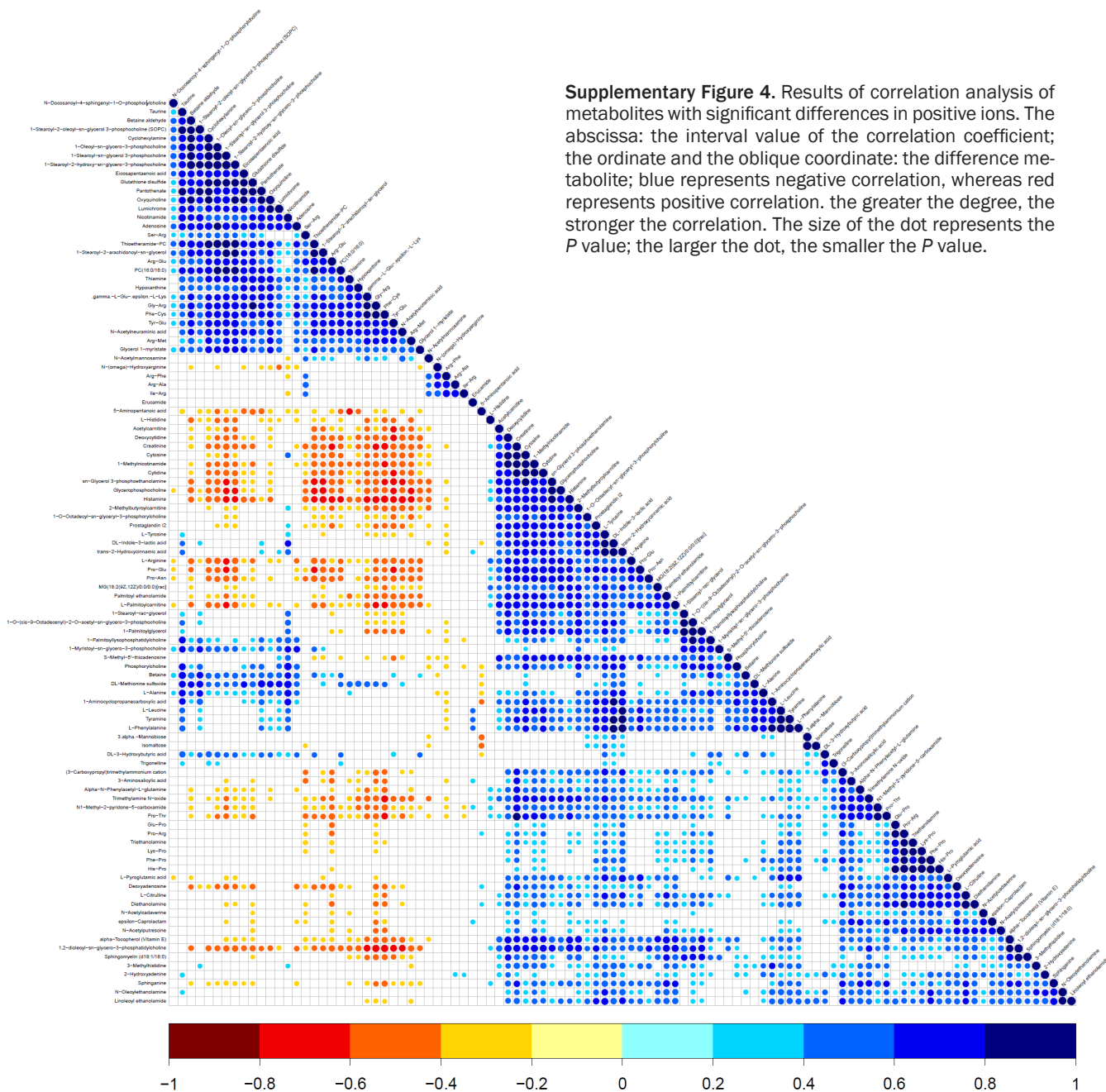
Supplementary Figure 2. Hierarchical clustering results of metabolites with significant differences in positive ions. Hierarchical clustering was performed on each group of samples by using the expression level of qualitative significant difference metabolites to assist in the screening of marker metabolites. When the selected candidate metabolites are reasonable and accurate, the same group of samples can appear in the same cluster through clustering. At the same time, metabolites clustered in the same cluster have similar expression patterns and may be in a relatively close reaction step in the metabolic process. The Red is positively correlated with its degree; The Blue is negatively correlated with its degree; the greater the degree, the stronger the correlation. R, stage 5 chronic kidney disease patients on hemodialysis; C, controls. The abscissa represents grouping; the right ordinate represents differential metabolites.

Stage 5 CKD oral microbiota and metabolites

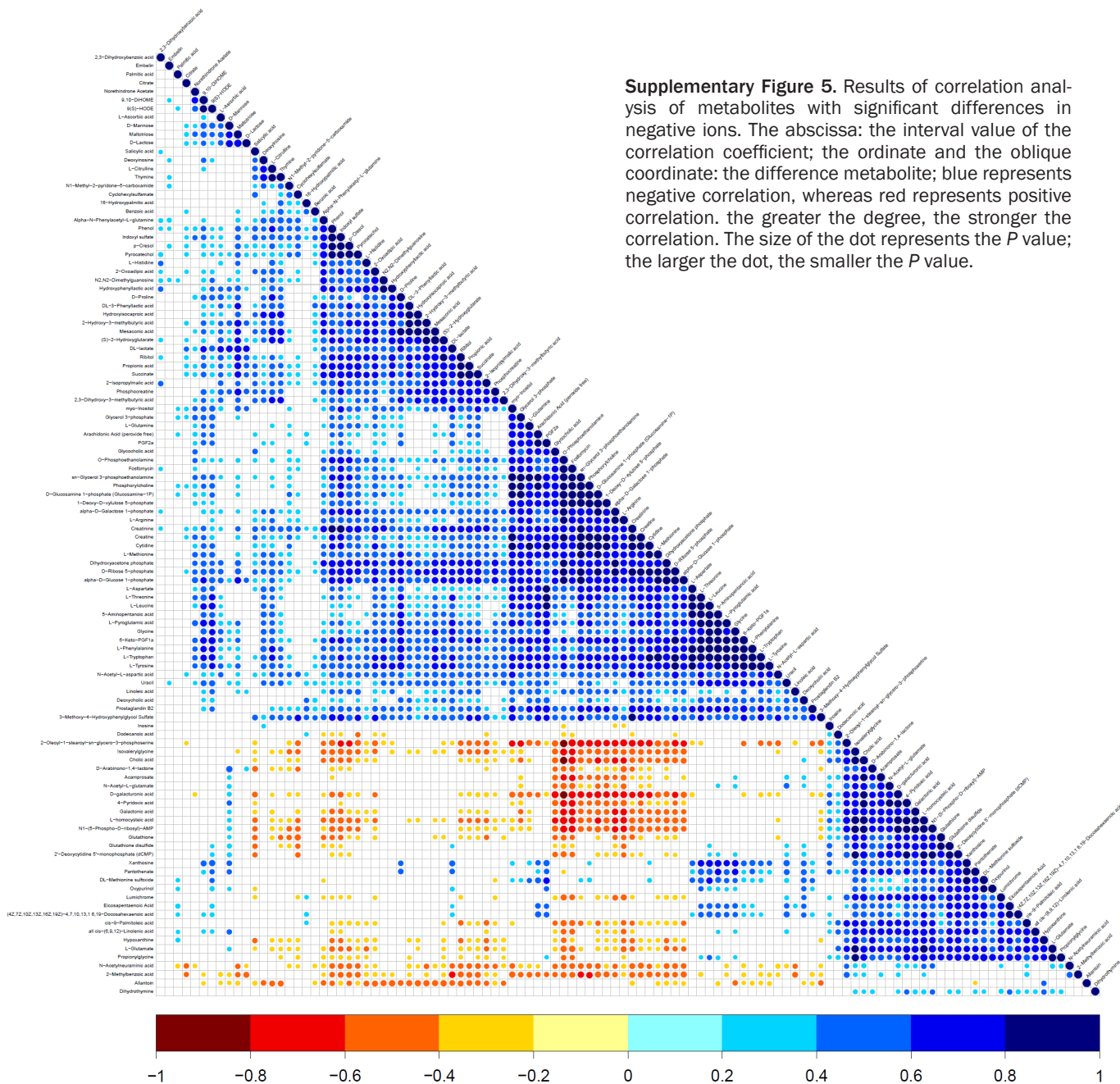


Supplementary Figure 3. Hierarchical clustering results of metabolites with significant differences in negative ions. Hierarchical clustering was performed on each group of samples by using the expression level of qualitative significant difference metabolites to assist in the screening of marker metabolites. When the selected candidate metabolites are reasonable and accurate, the same group of samples can appear in the same cluster through clustering. At the same time, metabolites clustered in the same cluster have similar expression patterns and may be in a relatively close reaction step in the metabolic process. The Red is positively correlated with its degree; The Blue is negatively correlated with its degree; the greater the degree, the stronger the correlation. R, stage 5 chronic kidney disease patients on hemodialysis; C, controls. The abscissa represents grouping; the right ordinate represents differential metabolites.

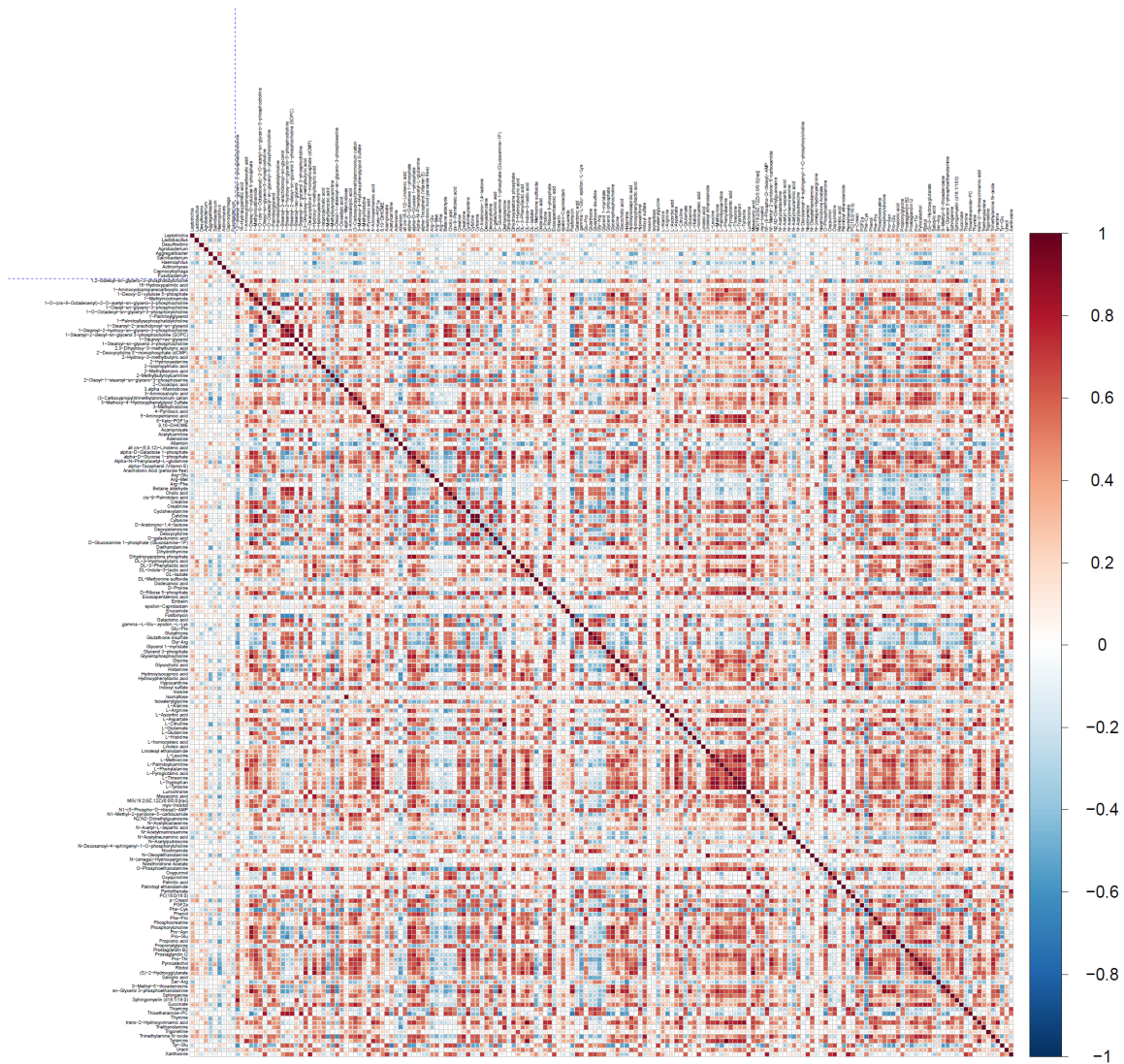
Stage 5 CKD oral microbiota and metabolites



Stage 5 CKD oral microbiota and metabolites

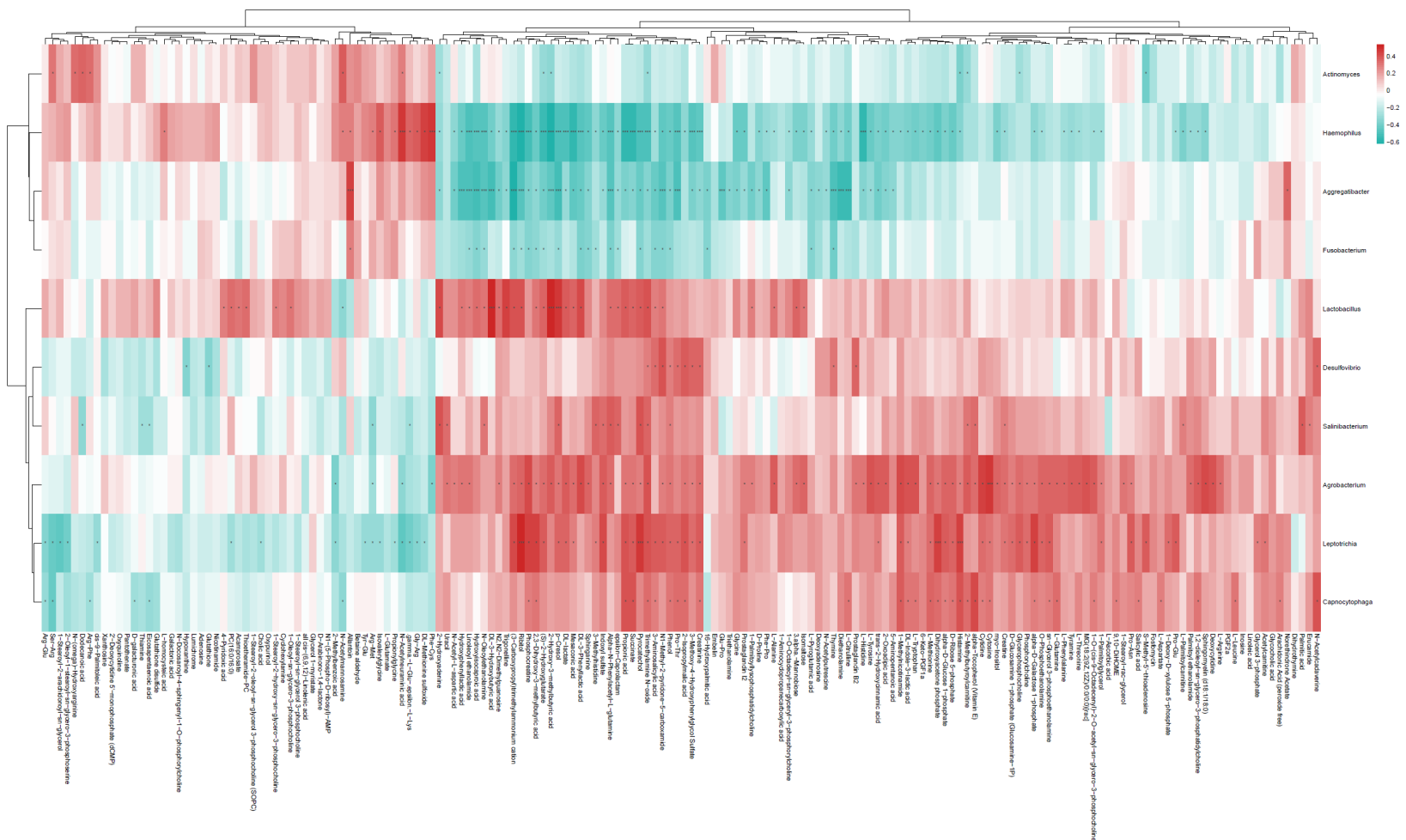


Stage 5 CKD oral microbiota and metabolites



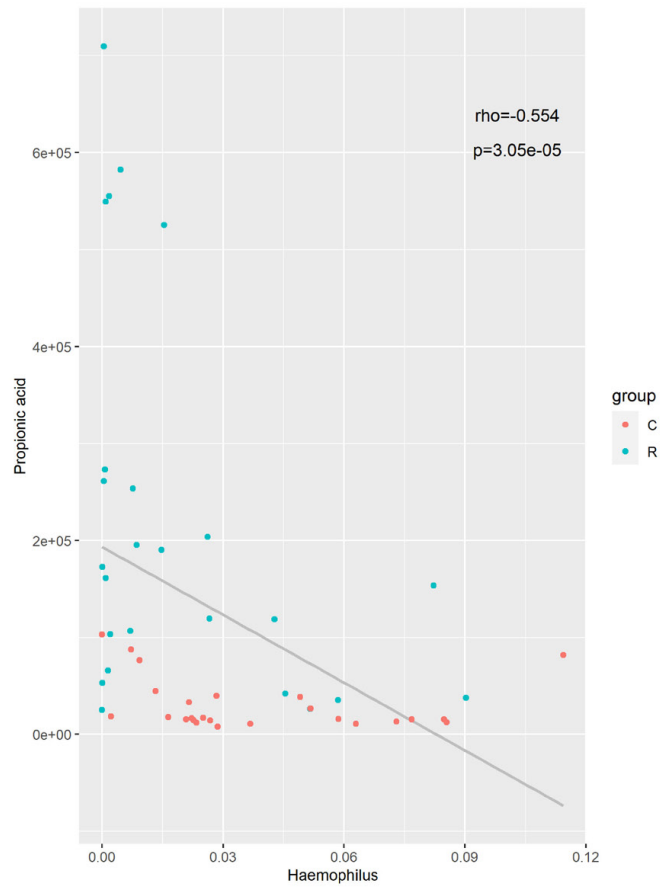
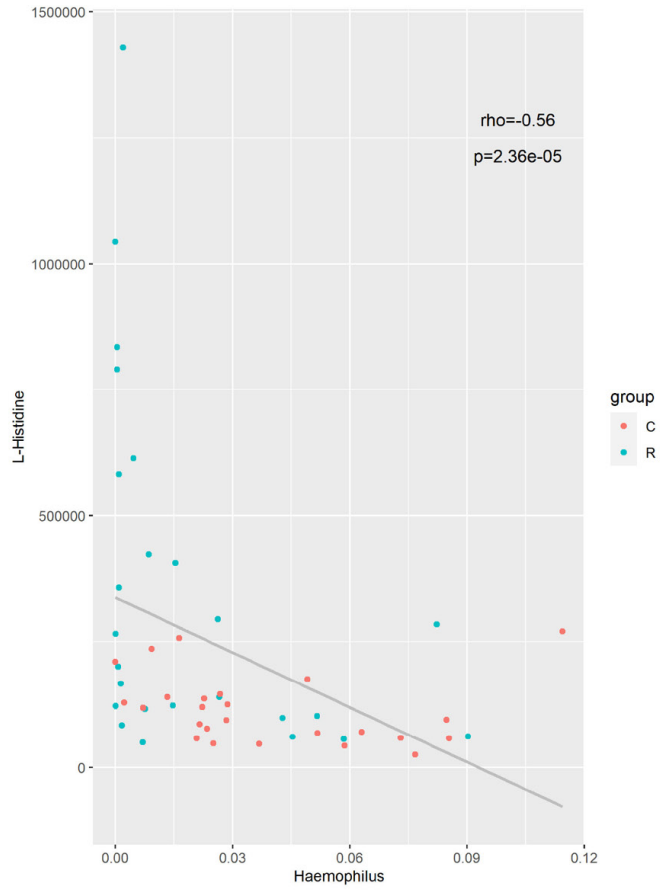
Supplementary Figure 6. Heat map of the spearman correlation coefficient matrix of the significantly different flora and the significantly different metabolites. Taking the blue dashed line as the dividing line in the figure, the correlation coefficient matrix heat map can be divided into four quadrants. The upper left corner shows the correlation between the significantly different bacterial groups; the lower right corner shows the correlation between the significantly different metabolites. The upper right corner and the lower left corner show the correlation between the significantly different flora and the significantly different metabolites, which are mirror symmetry. The Spearman correlation coefficient r is between -1 and $+1$. r is expressed in color. $r > 0$ indicates a positive correlation, which is indicated in red. The darker the color, the stronger the correlation.

Stage 5 CKD oral microbiota and metabolites

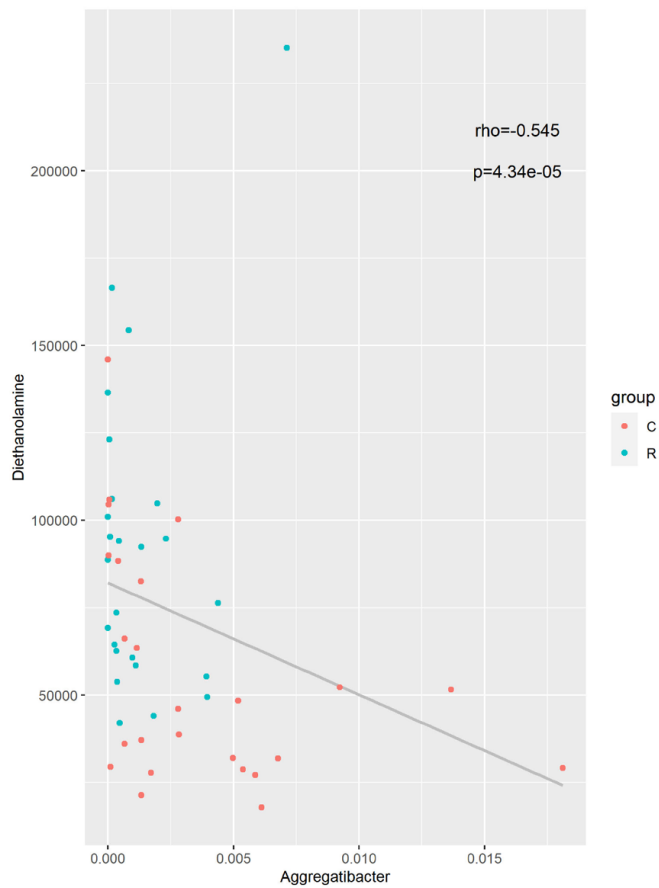
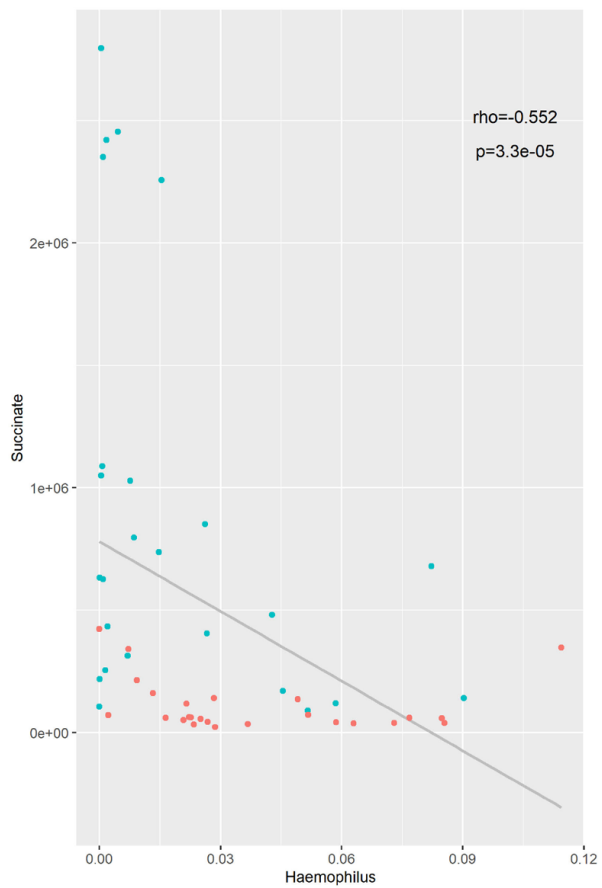


Supplementary Figure 7. Hierarchical clustering heat map of spearman correlation analysis between significant difference flora and significant difference metabolites. Each row in the figure represents a significantly different genus, and each column represents a significantly different metabolite. The tree branch on the left represents the result of clustering the different genera, and the upper tree branch represents the result of the cluster analysis of the different metabolites. Clusters appearing in the same cluster with significantly different metabolites or different bacterial genera have similar correlation patterns. Each grid in the figure contains two kinds of information (correlation coefficient r and p value). r is expressed in color. $r > 0$ indicates a positive correlation, which is indicated in red. $r < 0$ indicates a negative correlation, which is indicated in blue. The darker the color, the stronger the correlation. p value reflects the significant level of correlation, $0.01 < p < 0.05$, expressed as *; $p < 0.01$, expressed as **. The figure shows 426 pairs of significantly correlated different bacterial genera and metabolites, of which 181 pairs have a $p < 0.01$, and the correlation is more significant.

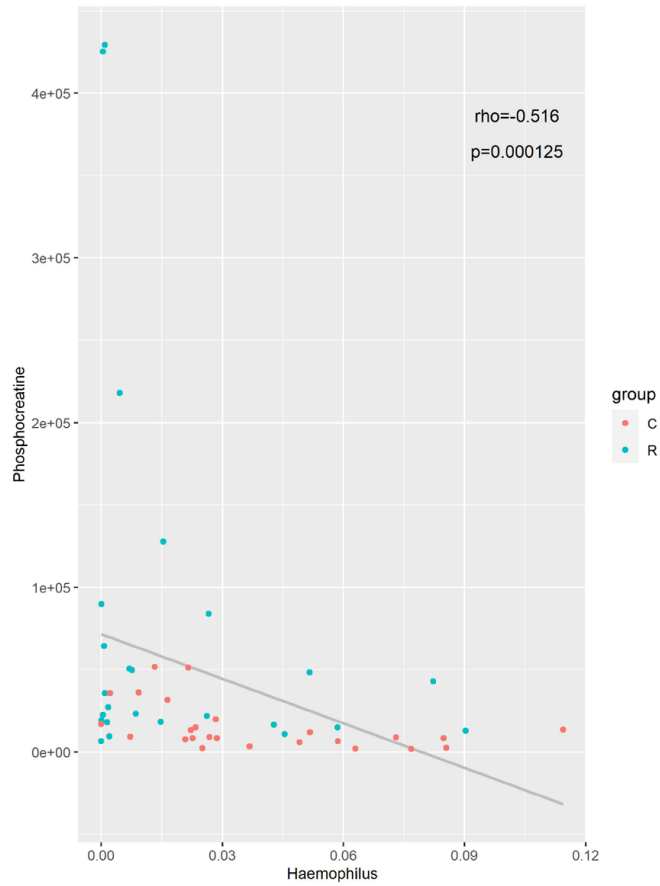
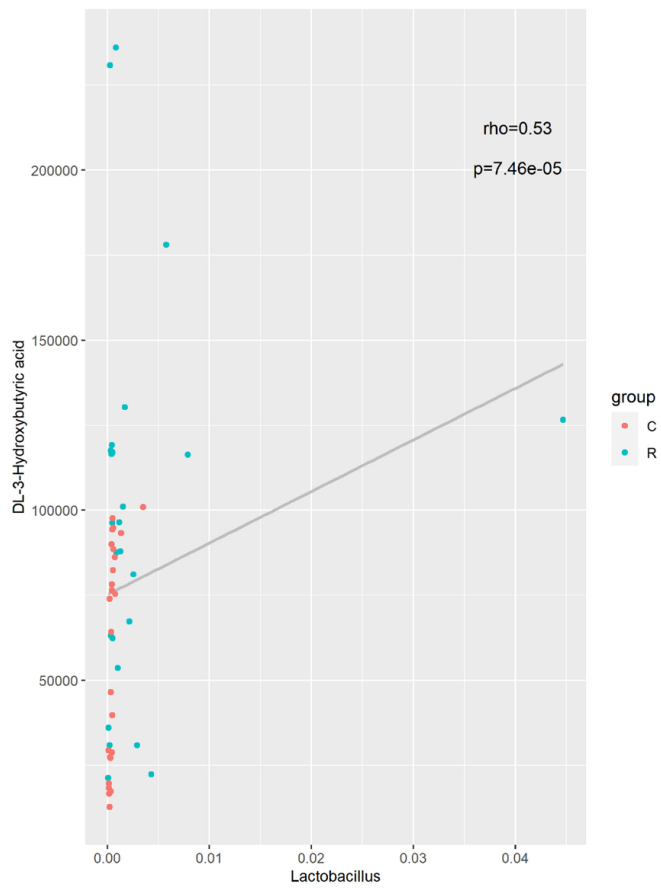
Stage 5 CKD oral microbiota and metabolites



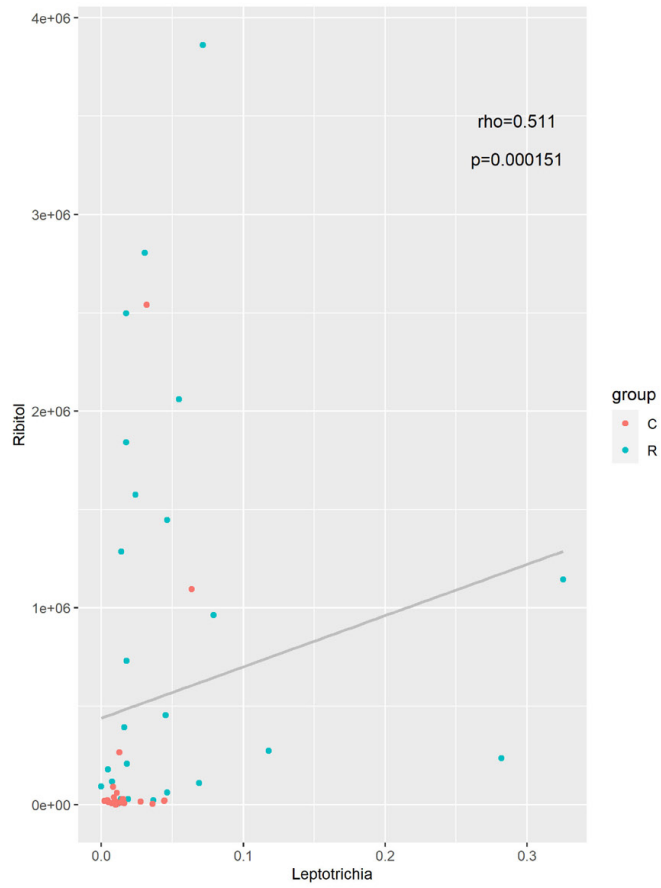
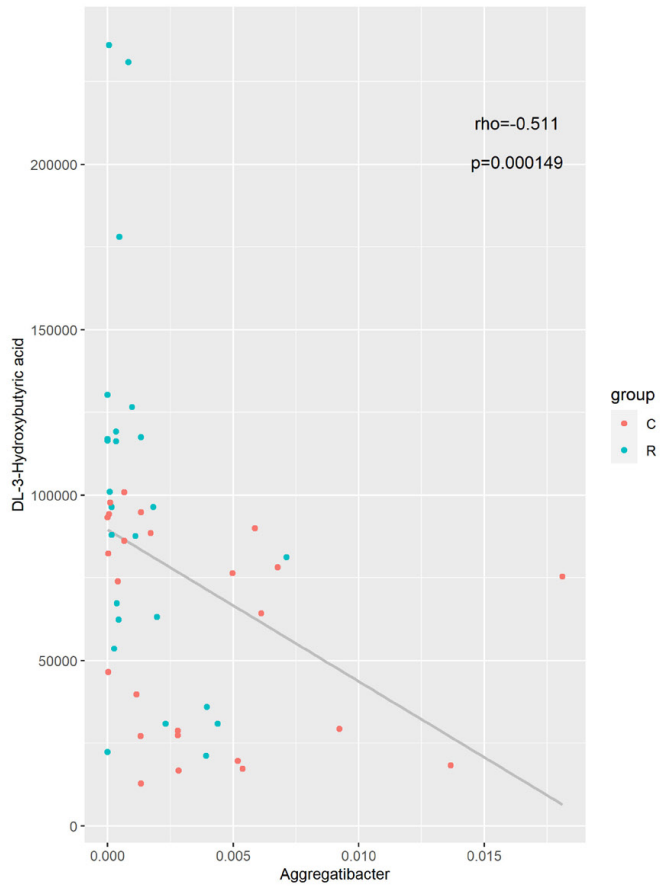
Stage 5 CKD oral microbiota and metabolites



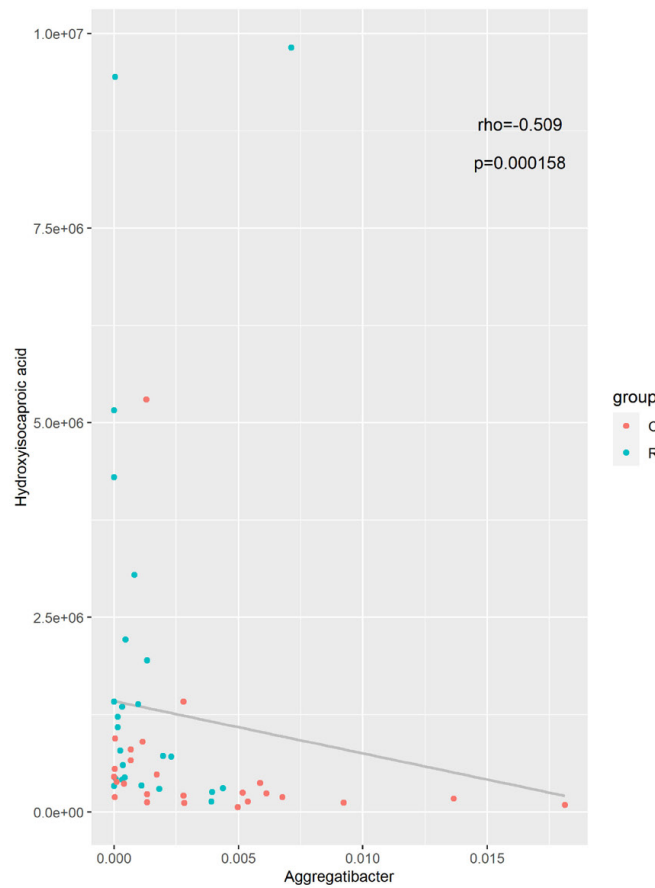
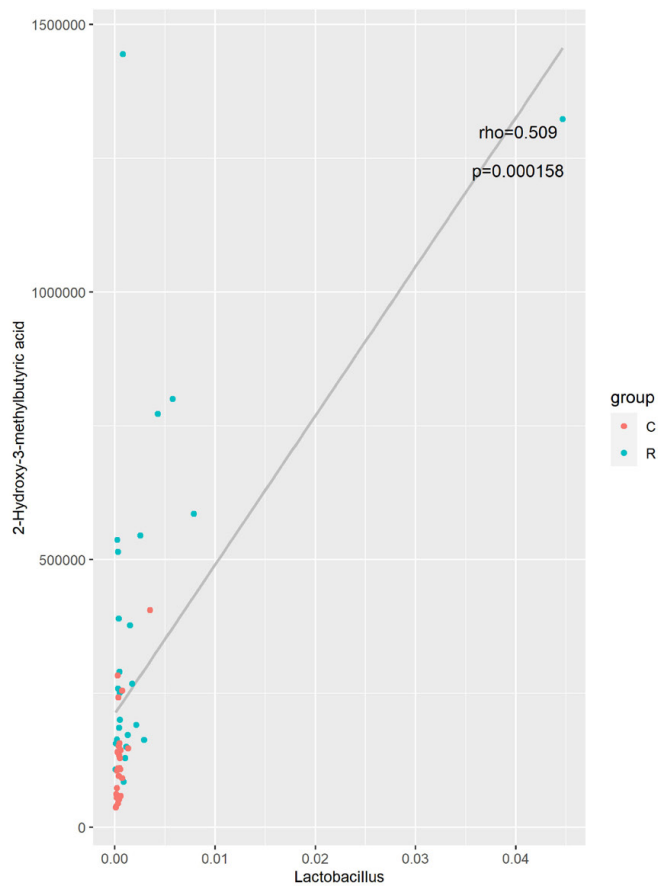
Stage 5 CKD oral microbiota and metabolites



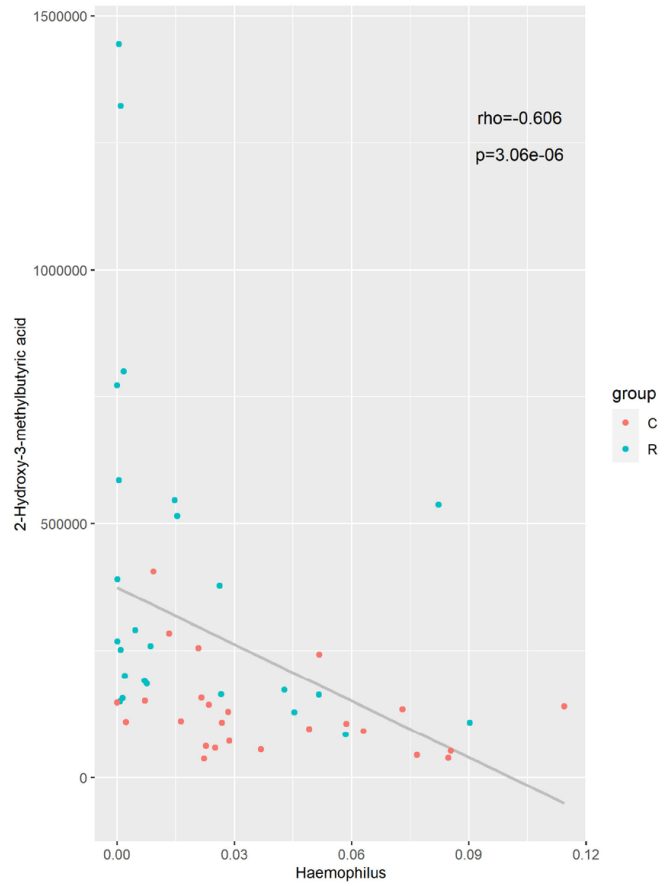
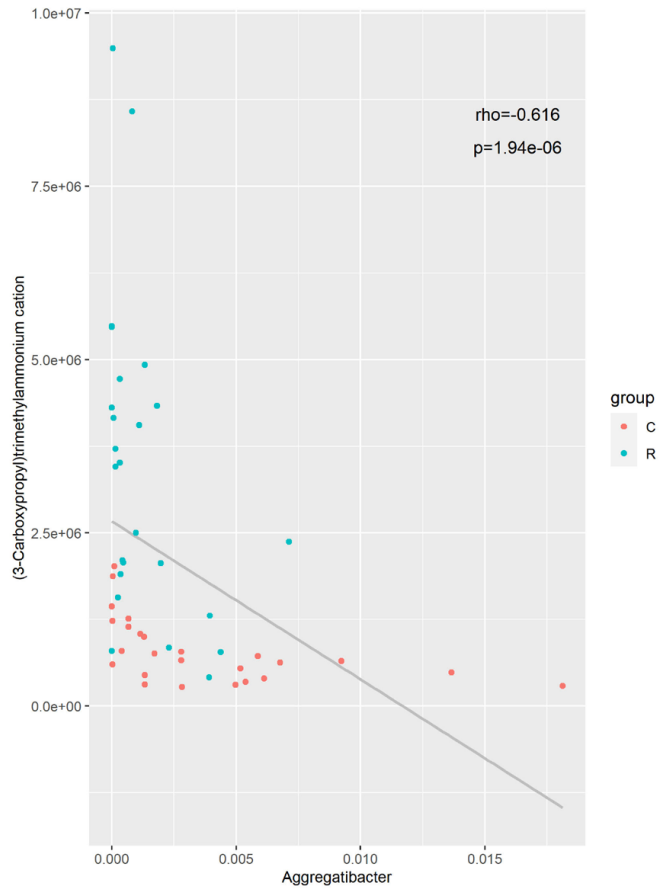
Stage 5 CKD oral microbiota and metabolites



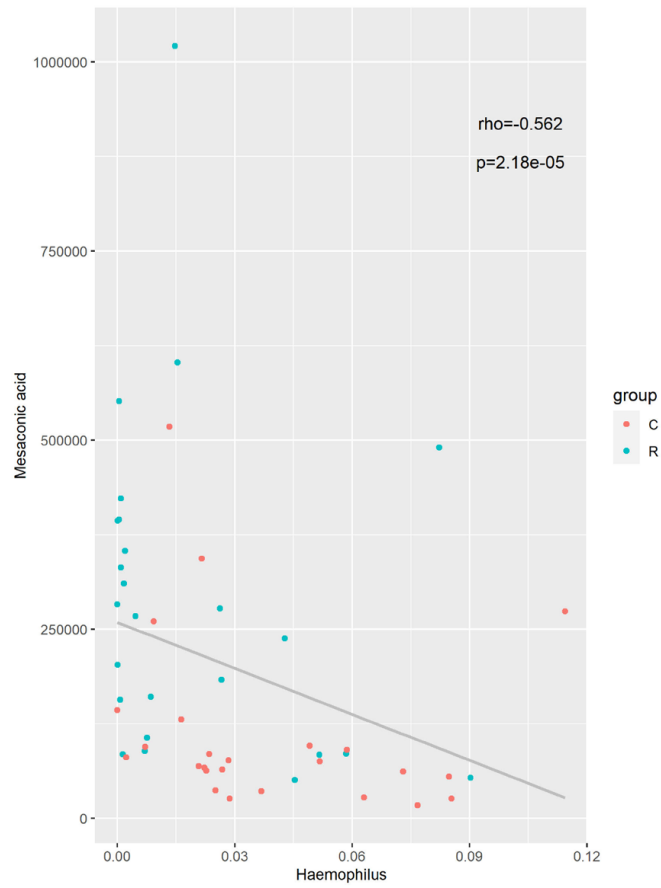
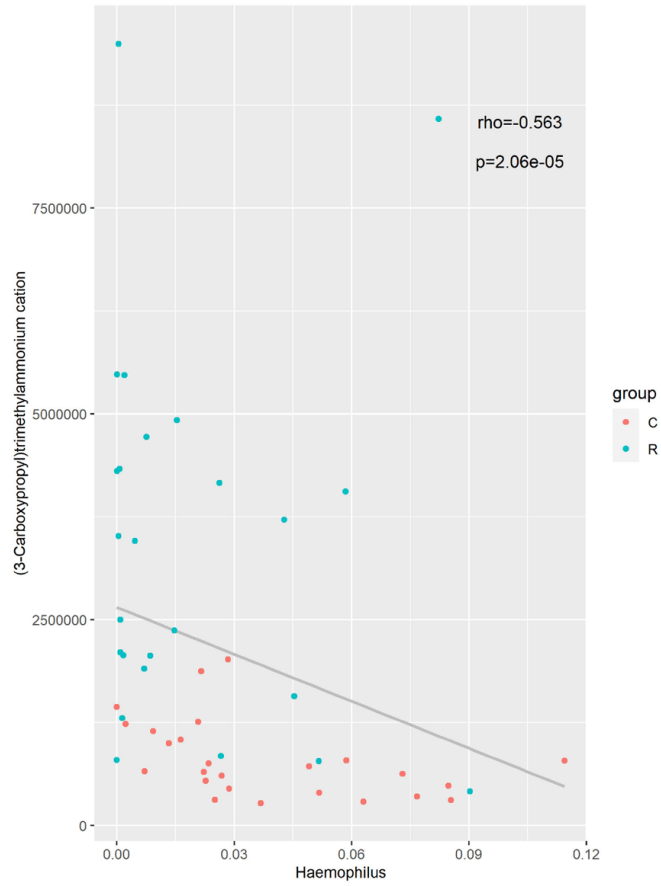
Stage 5 CKD oral microbiota and metabolites



Stage 5 CKD oral microbiota and metabolites



Stage 5 CKD oral microbiota and metabolites



Stage 5 CKD oral microbiota and metabolites

Supplementary Figure 8. Scatter plot of correlation. The scattered points in the figure represent samples, and the colors correspond to different grouping information. The rho shown in the upper left corner is the Spearman correlation coefficient between the relative abundance of the strain and the metabolite intensity; the p value is the significant level of the rho.